Basin scale distributions of dissolved manganese, nickel, zinc and cadmium in the Mediterranean Sea

Rob Middag [a,b,*], John M. Rolison [b,1], Ejin George [b], Loes J.A. Gerringa [a], Micha J. A. Rijkenberg [a], Claudine H. Stirling [b]

[a] Royal Netherlands Institute for Sea Research, Department of Ocean Systems (OCS), PO Box 59, 1790 AB Den Burg, Texel, the Netherlands
[b] Department of Geology and Centre for Trace Element Analysis, University of Otago, P.O. Box 56, Dunedin, New Zealand

ABSTRACT

Samples for dissolved trace metal concentrations were collected during GEOTRACES expedition GA04-N in summer/spring in the Mediterranean Sea, starting in the Atlantic Ocean and sampling both deep basins of the Mediterranean Sea. Outflow of Mediterranean Outflow Water leads to elevated concentrations of Mn, Ni and Zn in the Atlantic Ocean, but a concentration minimum in the Atlantic distribution of Cd. Nevertheless, when comparing the in- and outflow, the Mediterranean is a net source of Cd to the Atlantic Ocean. Surface concentrations of Mn, Ni, Zn and Cd are elevated in the Mediterranean relative to the Atlantic Ocean where Ni and Cd gradually increased along the eastward surface water flow path, Zn reached a homogenous concentration in the order of 1 to 1.5 nM, and Mn displayed a patchy surface distribution. The observed differences are attributable to the different dynamics of their biogeochemical cycling, notably the partitioning between the dissolved and particulate phases due to biological uptake, scavenging and possibly organic complexation. The elevated surface concentrations of Mn, Ni, Zn and Cd in the Mediterranean are derived from atmospheric deposition, where most likely Zn and Cd are mainly sourced from anthropogenic origin, Mn mostly from lithogenic origin and Ni from both anthropogenic and lithogenic origin. Dissolved Zn and Cd, as well as phosphate and nitrate, display striking inter-basin fractionations with elevated concentrations in the deep water of the western basin compared to the deep eastern basin, without a coinciding increase in the apparent oxygen utilization. Given that physical circulation or contribution from biogenic particulate metals cannot explain the elevated dissolved concentrations, an external non-biological source is required. This source is most likely a vertical flux of metal laden particles dissolving through the water column of the western Mediterranean where these particles, most likely from anthropogenic origin, are derived from either atmospheric deposition or particulate material deposited on the continental shelves that makes its way into the deep basin. To confirm or detect trends in dissolved metal concentrations in the deep basin, regular basin wide assessments of the trace metal distributions in the Mediterranean are needed. The distributions of Mn, Ni, Zn and Cd in the Sea of Marmara illustrate that all of these metals can be affected by anthropogenic surface sources and highlight the different susceptibilities of the dissolved metal distributions to supply from remineralization, and to removal through scavenging. This study provides a first baseline to assess future changes and underlines that the Mediterranean marine environment is susceptible to anthropogenic disturbances, with varying effects for different metals due to differing source strengths and biogeochemical cycles.

1. Introduction

Trace metals are essential nutrients to phytoplankton at the base of the marine food web, yet can also be toxic at high levels. Thus, the distributions of dissolved trace metals can significantly influence biological productivity. For example, availability of dissolved Fe limits primary productivity in high-nutrient low-chlorophyll (HNLC) regions, which account for over 30% of the world's ocean (e.g. Moore et al.,

---

2013). In the Mediterranean Sea, the supply of trace metals through atmospheric deposition is extremely high compared to the open ocean (e.g. Guerzoni et al., 1999) most likely ensuring that biological productivity is not limited by the availability of essential trace metals. More concerning for the Mediterranean Sea, however, are the effects of industrialization on the dissolved trace metal concentrations. As demonstrated by Jordi et al. (2012), the delivery of metal-laden aerosols to the surface ocean can have detrimental effects on phytoplankton communities within the Mediterranean Sea. It is, however, the dissolved species of trace metals that are generally bioavailable to marine biota and it is therefore important to understand the distributions of dissolved trace metals in the Mediterranean Sea in order to assess how they might influence modern marine ecosystems.

The Mediterranean Sea is a semi-enclosed marine basin that, despite being oligotrophic, supports diverse ecosystems that are of vital socio-economic importance to the many countries that border its shores (UNEP, 2005). The small size and, as the name implies, enclosed nature of the Mediterranean Sea, make it especially vulnerable to environmental change, such as changing climate and intensified metal pollution (Durrieu de Madron et al., 2011). Elevated concentrations of trace metals with known anthropogenic sources to the environment, such as cadmium (Cd) and zinc (Zn), have been observed in the water column (e. g. Boyle et al., 1985; Morley et al., 1997; Statham et al., 1985; Van Geen et al., 1991), marine sediments (e.g. Alonso Castillo et al., 2013; Cossa et al., 2014; Martín et al., 2009) and marine organisms (e.g. Benedicto et al., 2011; Copat et al., 2012; Yilmaz, 2003) at different locations in the Mediterranean Sea. These observations indicate that anthropogenic activities significantly impact the trace metal fluxes to coastal zones of the Mediterranean Sea. The delivery of trace metals from natural or anthropogenic sources to the Mediterranean Sea is thought to be dominated by atmospheric transport processes and by continental runoff, but submarine groundwater discharge could play a role too (Rodellas et al., 2015), notably in coastal regions (Trezzi et al., 2016). Rivers receive and transport trace metals derived from various anthropogenic and natural sources including agricultural runoff (Dumas et al., 2015), urban runoff (Nicolau et al., 2012), industrial effluent, acid mine drainage (Nieto et al., 2007) and treated wastewater discharge (Oursel et al., 2013). In contrast to these point sources, the atmospheric transport of natural and anthropogenic aerosols delivers trace metals to surface waters throughout the Mediterranean (e.g. Guieu et al., 1997; Guieu et al., 2010). The use of a three-dimensional atmospheric chemistry transport model implies significant increases in the atmospheric deposition of soluble nitrogen (N), phosphorus (P) and iron (Fe) as the result of the increase in anthropogenic and biomass burning emissions (Kanakidou et al., 2020), but consequences for the distributions of metals in general are unknown.

Although much work has been done focusing on the sources of trace metals to the Mediterranean Sea and the accumulation of trace metals in sediments, there has been less focus on the distributions of dissolved trace metals, due to the challenging sampling and analytical methods required for acquiring reliable open ocean dissolved trace metal concentrations. This hinders our ability to understand the cycling of metals and the influence of pollution in this vital marine basin. However, recent efforts within the GEOTRACES programme have highlighted the significant influence of atmospheric, riverine and margin fluxes for cobalt (Dulaquais et al., 2017). For Fe and aluminium (Al), atmospheric deposition is deemed the most important surface source, whereas in the deep ocean, mud volcanoes are a source of Fe and interaction with topography constitutes a source of both Al and Fe (Gerringa et al., 2017; Rolison et al., 2015). Here we report concentration data from the GA04-N GEOTRACES zonal transect in the Mediterranean Sea on the distributions of dissolved manganese (Mn), nickel (Ni), Zn and Cd. These elements were chosen as they are all bio-essential (Mn, Ni and Zn) or bio-active (Cd) where especially Zn and Cd have a strong anthropogenic source component, whereas Mn has a mainly lithogenic origin and Ni a mix of anthropogenic and lithogenic sources (Heimbürger et al., 2010).

This study was designed to gain a basin wide overview of the distribution of the metals and address the first order processes that govern these distributions. The data reveal a striking enrichment of anthropogenic dissolved trace metals in the deep western Mediterranean basin, relative to the known primary sources of water to the western Mediterranean, which are Atlantic Ocean surface waters and intermediate and deep waters formed in the eastern Mediterranean basin.

2. Methods

2.1. Study region

Samples were collected during GEOTRACES expedition GA04-N in two legs, 64PE370 (Lisbon-Istanbul) and 64PE374 (Istanbul-Lisbon), in the Mediterranean Sea aboard RV Pelagia during May-June 2013 and July-August 2013, respectively (Fig. 1). All stations were sampled for dissolved trace metals with the exception of stations 25 and 37 during leg 64PE370 and station 16 during 64PE374. Expedition 64PE370 followed a west to east transect from the Atlantic Ocean to the eastern Mediterranean basin before turning north through the Aegean Sea and will be described as the southern transect and stations denoted as S.n where n is the station number. Specifically, stations S.1 to S.4 were in the Atlantic Ocean, stations S.5 to S.12 were in the western Mediterranean basin, stations S.13 to S.15 were across the Channel of Sicily with bottom depths shallower than 1000 m (sill depth ~ 300 m), and stations S.16 to S.28 were in the eastern Mediterranean basin with station S.23 being the most eastward. Stations S.29 to S.37 were in the Aegean Sea and the Sea of Marmara. Expedition 64PE374 generally followed an east to west transect beginning in the southern Aegean Sea and ending in the western Mediterranean basin and will be described as the northern transect, with stations denoted as N.n. Specifically, station N.1 was located in the southernmost region of the Aegean Sea, just to the north of the isle of Crete. Stations N.2 to N.11 were in the eastern Mediterranean basin and southern Adriatic Sea, stations N.12 to N.15 were in the Tyrrhenian basin, and stations N.16 to N.19 were in the western Mediterranean basin.

2.2. Sample collection

Seawater samples were collected using an ultraclean all-titanium CTD sampling system (De Baar et al., 2008) outfitted with 24 × 24 L Pristine sample bottles constructed from ultrapure polyvinylidene fluoride (PVDF) and titanium (Rijkenberg et al., 2015). Immediately upon recovery, the system was placed inside a purpose-built, positive pressure, clean air sampling container. Inside this clean room container, seawater was filtered directly from the Pristine samplers using 0.2 μm filter cartridges (Sartobran-300, Sartorius) under nitrogen overpressure (~0.5 atm) and hence all data presented here concern dissolved metals. Samples were collected in 60 mL low density polyethylene (LDPE)
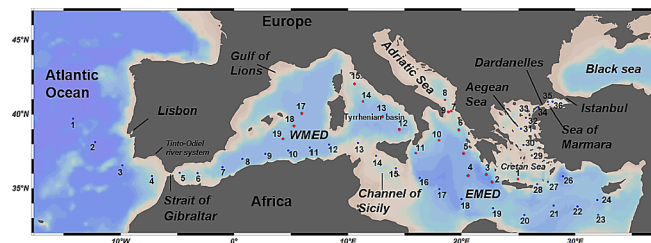
Fig. 1. Map of the sampling region for GEOTRACES expedition GA04-N during 2 legs, 64PE370 (Lisbon-Istanbul) and 64PE374 (Istanbul-Lisbon), in the Mediterranean Sea aboard RV Pelagia during May-June 2013 and July-August 2013. Stations along the southern transect are denoted in blue and stations along the northern transect are shown in red. (For interpretation of the references to color in this figure legend, the reader is referred to the web version of this article.)

bottles (Nalgene, Fisher Scientific) that were rigorously acid cleaned following GEOTRACES protocols. Immediately after collection, samples were acidified to 0.024 M HCl using ultra-high purity 12 M HCl (Seastar Baseline).

2.3. Hydrographic data and nutrients

A Seabird SBE 911+ CTD system was used to measure the conductivity (salinity), temperature, pressure (depth), and dissolved oxygen in situ at each station as detailed and reported by Gerringa et al. (2017). Samples for the macro nutrients phosphate (PO_4), silicate (Si), nitrate (NO_3) and nitrite (NO_2) were collected unfiltered in a 5 mL polyethylene vial and stored at 4 °C until analysis. All samples were analysed colorimetrically (Grasshoff et al., 1983) within 18 h after collection on a QuAAtro autoanalyzer. Detection limits, defined as 2.82 * standard deviation of 10 samples containing 0.06, 1.6, 0.34 and 0.02 μM (2% of the highest standard used for the calibration curve), were 0.008, 0.014, 0.011 and 0.007 μM, respectively for PO_4, Si, $NO_3 + NO_2$ (combined) and NO_2. A sterilised natural Reference Nutrient Sample (Kanso, Lot code BU) containing known concentrations of nutrients, was analysed in triplicate every run. The precision (1 SD) was around 1% of the average value and there was no significant difference between the shipboard measured values of Kanso and the consensus values. The deepest sample analysed for a station of 24 samples, was kept and re-analysed within the next run of the next station of 24 samples as verification for variability between runs. This resulted in absolute deviations of 0.5%, 0.2%, 0.1% and 8.6% at average concentrations of 0.237 μM PO_4, 7.29 μM Si, 5.81 μM $NO_3 + NO_2$ (combined) and 0.03 μM NO_2, respectively.

2.4. Shipboard pre-concentration of metals

Detailed descriptions of the methods used for pre-concentrating trace metals from seawater are presented by Biller and Bruland (2012) and Middag et al. (2015). Slight modifications were made in order to make the methods more amenable to working while at sea. Briefly, a version of the off-line pre-concentration system described by Biller and Bruland (2012), which employs the Nobias-PA1 chelating resin to extract trace metals from seawater, was installed in a laminar flow bench inside a laboratory container aboard RV Pelagia. The system was composed of 8 individual micro-columns (~40 μL resin bed) and was therefore capable of pre-concentrating 8 samples simultaneously. The seawater samples remained acidified for at least 5 h before the pre-concentration procedure was commenced. Exactly 40 mL of acidified seawater was then volumetrically transferred from the original 60 mL LDPE sample bottle into a second acid cleaned 40 mL LDPE using a 10 mL pipette. The 40 mL sample was then spiked with 50 μL of a Lu—In spike (resulting in a final concentration of 5 nM for both Lu and In in the final 40 mL sample assuming negligible Lu and In in open ocean seawater), which served as internal standards, allowing for the calculation of the concentration of trace metals present in seawater based on an 'element dilution' approach (see Middag et al. (2015) for further details). The samples were then allowed 2 h to equilibrate before metal extraction. Immediately prior to the extraction, 20 μL of 1.2 M HF was added and the pH of the samples was adjusted to 5.8 ± 0.2 with ~500 μL of a 3.7 M ammonium acetate (NH_4Ac) buffer. Trace metals were then extracted by passing ~35 mL of the buffered samples across columns packed with precleaned Nobias resin. After loading of the sample, the columns were rinsed with 0.05 M NH_4AC to remove major cations before elution. The metals remaining on the column were then eluted in ~2 mL of 1 M HNO_3 containing 10 ng g^{-1} Rh which was used to monitor instrumental drift (described below). The eluent acid was collected in 8 mL acid cleaned LDPE bottles. The pre-concentration method results in a concentration factor of ~17.5 and the removal of >99.9% of salts present in the original seawater sample, allowing for the analysis of a suite of trace metals by high resolution ICP-MS, as described below.

The pre-concentration method was calibrated following the standard addition approach. A multi-elemental stock standard containing Ti, Mn, Fe, Co, Ni, Cu, Zn, Y, Cd, La and Pb with natural isotopic abundances was added to natural seawater containing low concentrations of metals. Five standard additions were used for the construction of the calibration curve. The standards were also spiked with the Lu—In spike to a concentration of 5 nM each. The standards were then processed alongside samples in an identical fashion. A standard addition calibration was performed approximately every 8 stations. The Mn, Ni, Zn and Cd will be discussed here while other metals are described separately. The metals Mn, Ni, Zn, Y, Cd, La and Pb have been intercalibrated and submitted to the GEOTRACES IDP and are either available in the 2017 version (Schlitzer et al., 2018) or will be part of the IDP 2021. Additionally, data for cobalt (Dulaquais et al., 2017) and Fe (Gerringa et al., 2017) determined using different methods have been published and are available in the IDP.

The performance of the shipboard pre-concentration method was verified and validated by processing SAFe Surface and Deep reference samples along with every calibration. The trace metal concentrations in these reference materials analysed by the shipboard pre-concentration method during the Dutch GEOTRACES expeditions to the Mediterranean and Black Sea in 2013 (expeditions 64PE370, 64PE373, and 64PE374) were in good agreement with the GEOTRACES consensus values (Table 1). Furthermore, 4 × 1 L samples of Mediterranean Outflow Water collected at station N.1 were sub-sampled and processed to assess the reproducibility of the method. Both the reference samples and the MOW sample were processed with every calibration (approximately every 8 stations). In total, the Mediterranean Outflow Water in-house reference sample was processed 32 times and the average concentration and standard deviation of the analysed elements are shown in Table 2. The results of these reference materials demonstrate that the shipboard pre-concentration with 'element dilution' method and subsequent ICP-MS analysis produces accurate and reproducible concentrations of multiple dissolved trace metals.

2.5. Analysis by ICP-MS

The metal analysis protocol used in the present study is described in detail elsewhere (Biller and Bruland, 2012; Middag et al., 2015). Briefly, the pre-concentrated samples in ~2 mL of 1 M HNO_3 were analysed directly on a Thermo Element XR magnetic sector inductively coupled plasma mass spectrometer (ICP-MS) at the Institute of Marine Science, University of California, Santa Cruz. The ion beam intensities of $^{89}Y^+$, $^{111}Cd^+$, $^{139}La^+$, $^{208}Pb^+$, and $^{95}Mo^+$ were measured in low resolution mode, while the intensities of $^{47}Ti^+$, $^{55}Mn^+$, $^{56}Fe^+$, $^{59}Co^+$, $^{60}Ni^+$, $^{63}Cu^+$ and $^{66}Zn^+$ were measured in medium resolution. The ion beam

Table 1

Measured (average of $n = 8$) and consensus values of SAFe Surface (S), Deep (D) and GEOTRACES Surface Pacific (GSP) reference samples with 1SD uncertainty. Units are as indicated in the table to match the consensus values units as published on the GEOTRACES website (https://www.geotraces.org/standards-and-reference-materials/; September 2021).

	Mn (nmol/kg)	Ni (nmol/kg)	Zn (nmol/kg)	Cd (pmol/kg)
SAFe S1				
Measured	0.85 ± 0.03	2.23 ± 0.03	0.07 ± 0.02	1 ± 1
Consensus	0.79 ± 0.06	2.28 ± 0.09	0.069 ± 0.010	1.1 ± 0.3
SAFe D1				
Measured	0.40 ± 0.02	8.4 ± 0.3	7.5 ± 0.5	957 ± 18
Consensus	NA	8.58 ± 0.26	7.40 ± 0.35	991 ± 31
SAFe D2				
Measured	0.42 ± 0.01	8.5 ± 0.3	7.4 ± 0.3	958 ± 13
Consensus	0.79 ± 0.06	8.63 ± 0.25	7.43 ± 0.25	986 ± 23
GSP				
Measured	0.77 ± 0.04	2.4 ± 0.2	0.03 ± 0.02	2 ± 2
Consensus	0.78 ± 0.04	2.6 ± 0.1	0.03 ± 0.05	2 ± 2

Table 2
Results obtained for the Mediterranean Overflow Water in-house reference sample (n = 32).

	Mn (nM)	Ni (nM)	Zn (nM)	Cd (pM)
Average	0.26	3.86	1.96	192
1 SD	0.02	0.09	0.09	3
RSD (%)	7%	2%	5%	2%

intensities of $^{115}In^{+}$, $^{175}Lu^{+}$, and $^{103}Rh^{+}$ were measured in both low and medium resolution. The presence of Rh in the elution acid was used to quickly detect any sample uptake problems and monitor changes in the instrumental sensitivity during the run, whereas In and Lu were used as internal standard (Middag et al., 2015). The presence of the polyatomic interference of $^{95}Mo^{16}O^{+}$ on $^{111}Cd^{+}$ was corrected by monitoring $^{95}Mo^{+}$ and calculating an oxide production rate based on Mo standards (Biller and Bruland, 2012). All samples, standards, blanks and reference materials which were processed using the shipboard pre-concentration method during the Dutch GEOTRACES expeditions in 2013 to the Mediterranean (expeditions 64PE370 and 64PE374) and Black Seas (expedition 64PE373) were analysed during one analytical session on the ICP-MS (~150 h total instrument time required for the analysis of ~2100 samples, standards, blanks, and reference samples). Roughly halfway through this session, the initial sensitivity for Rh had dropped by 25% after which the run was paused to clean the cones and re-tune the instrument.

3. Results

3.1. General hydrography

The thermohaline circulation in the Mediterranean Sea is complex and there are numerous reviews which cover the topic in detail (e.g. Kassis and Korres, 2020; Millot and Taupier-Letage, 2005; Skliris, 2014). The hydrography along the GA04-N GEOTRACES zonal transect has been described before (Dulaquais et al., 2017; Gerringa et al., 2017; Rolison et al., 2015) and is briefly summarized here. The Mediterranean Sea is a concentration basin (evaporation exceeds precipitation and runoff) and is connected to the Atlantic Ocean via the Strait of Gibraltar (Fig. 1). Due to net evaporation, the sea surface height of the Mediterranean Sea is slightly lower than the Atlantic Ocean, thereby promoting the inflow of surface Atlantic Water (AW;(Millot and Taupier-Letage, 2005)). The general flow path of AW can be tracked by a salinity minimum in surface Mediterranean waters (Fig. 2). The salinity of AW is ~36 as it enters the western Mediterranean basin (WMED), while the salinity of surface waters in the eastern Mediterranean basin (EMED) reaches >39. The salinity gradient in Mediterranean surface waters is a result of mixing between inflowing low salinity AW with high salinity Mediterranean waters and net evaporation. The high salinity surface waters of the EMED, periodically promote the formation of Levantine Intermediate Water (LIW) during winter time cooling. A second intermediate water mass formed in the EMED known as Cretan Intermediate Water (CIW), is less saline yet denser than LIW (colder) and is produced in smaller volume than LIW (Velaoras et al., 2014). We note that LIW and CIW are difficult to distinguish from each other based on thermohaline characteristics alone and thus LIW is often used to denote all intermediate water present in the EMED and WMED. After formation, LIW spreads throughout the entire EMED and WMED and can be identified as a subsurface salinity maximum in the upper ~300 m in the EMED and across a depth range between ~200 and 600 m in the WMED before it eventually flows out of the Mediterranean Sea as the primary component of Mediterranean Outflow Water (MOW; Fig. 2). The core of MOW can be tracked as it spreads through the North Atlantic Ocean by a mid-depth salinity maximum centred around 1250 m. Deep water formation can also occur during winter time cooling in the northern regions of the Mediterranean Sea. In the WMED, Western Mediterranean Deep
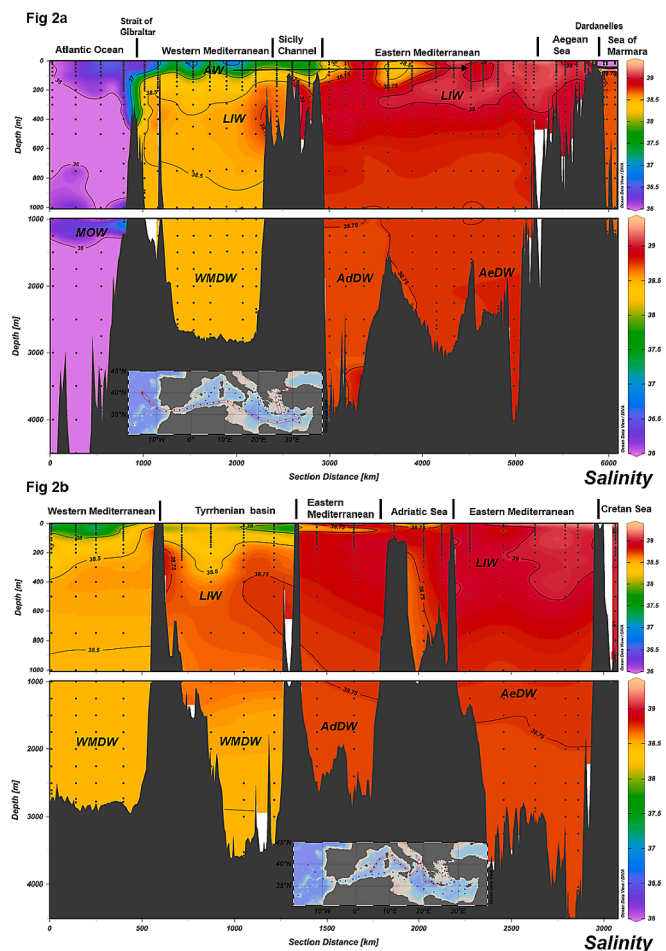

Fig. 2. Distribution of salinity in color scale. 2a Salinity along the Southern transect in the upper 1000 m (upper panel) and the remainder of the water column (lower panel). 2b Salinity along the northern transect in the upper 1000 m (upper panel) and the remainder of the water column (lower panel). The arrow indicates the direction of advection of Atlantic Water. Abbreviations: AW: Atlantic Water; AdDW: Adriatic Deep Water; AeDW: Aegean Deep Water; LIW: Levantine Intermediate Water; MOW: Mediterranean Outflow water; WMDW: Western Mediterranean Deep Water.

Water (WMDW) is the only significant deep water and primarily forms in the region of the Gulf of Lions (Fig. 1) where a ventilation event was observed in the winter prior to the current observations (Testor et al., 2018). In the EMED, deep water mainly forms in the southern Adriatic Sea (Fig. 1), but also forms in the southern Aegean Sea (Fig. 1) under certain environmental conditions. Between 2012 and 2017, there was intense dense water production in the Adriatic Sea, while the Aegean Sea underwent a relaxation phase (Kassis and Korres, 2020). In the deep EMED, Adriatic Deep Water (AdDW) can be identified as the water mass with a salinity of <38.75, while Aegean Deep Water (AeDW) has a salinity >38.75 (Fig. 2). Deep waters exiting the EMED at the Sicily Channel is termed Eastern Mediterranean Deep Water (EMDW) and consists of contributions from both AdDW and AeDW.

3.2. Zonal distribution of dissolved Mn, Ni, Zn and Cd

The full depth zonal distributions of dissolved Mn (Fig. 3), Ni (Fig. 4), Zn (Fig. 5) and Cd (Fig. 6) reveal enrichments of Ni and Zn in the Mediterranean relative to similar depths in the Atlantic whereas deep concentrations of Cd and Mn were comparatively low. Moreover, within the Mediterranean Sea itself, there was a clear enrichment of dissolved Zn and Cd in the deep (deeper than 300 m) WMED relative to the EMED,

Fig. 3. Distribution of manganese in color scale. 3a Concentration of dissolved Mn (nM) along the Southern transect in the upper 1000 m (upper panel) and the remainder of the water column (lower panel). 3b Concentration of dissolved Mn (nM) along the northern transect in the upper 1000 m (upper panel) and the remainder of the water column (lower panel). Abbreviations as in Fig. 2.

whereas for dissolved Ni and Mn there were no stark contrasts between the deep EMED and deep WMED.

3.2.1. Dissolved Mn

In the oceans, dissolved Mn has a typical scavenged type vertical profile with elevated concentrations near the surface that decreased to low and relatively uniform concentrations in the deep ocean (Bruland

Fig. 4. Distribution of nickel in color scale. 4a Concentration of dissolved Ni (nM) along the Southern transect in the upper 1000 m (upper panel) and the remainder of the water column (lower panel). 4b Concentration of dissolved Ni (nM) along the northern transect in the upper 1000 m (upper panel) and the remainder of the water column (lower panel). Abbreviations as in Fig. 2.
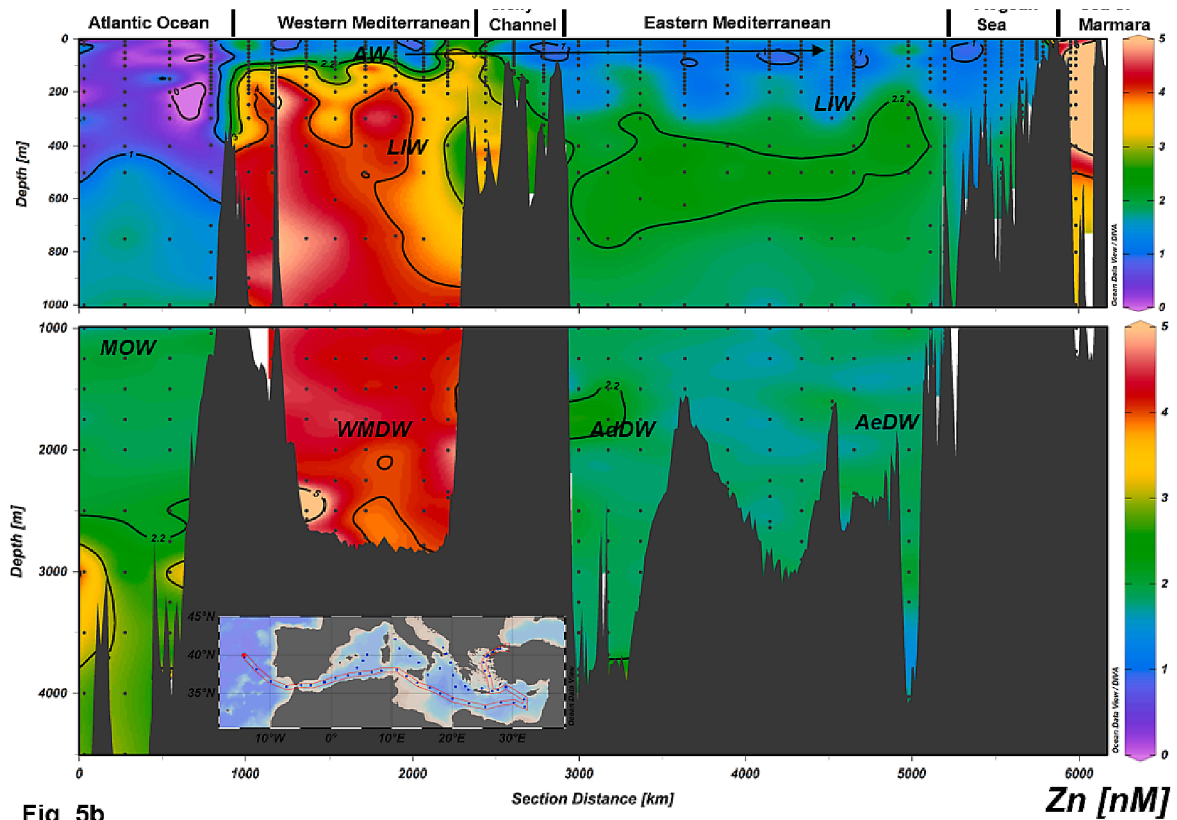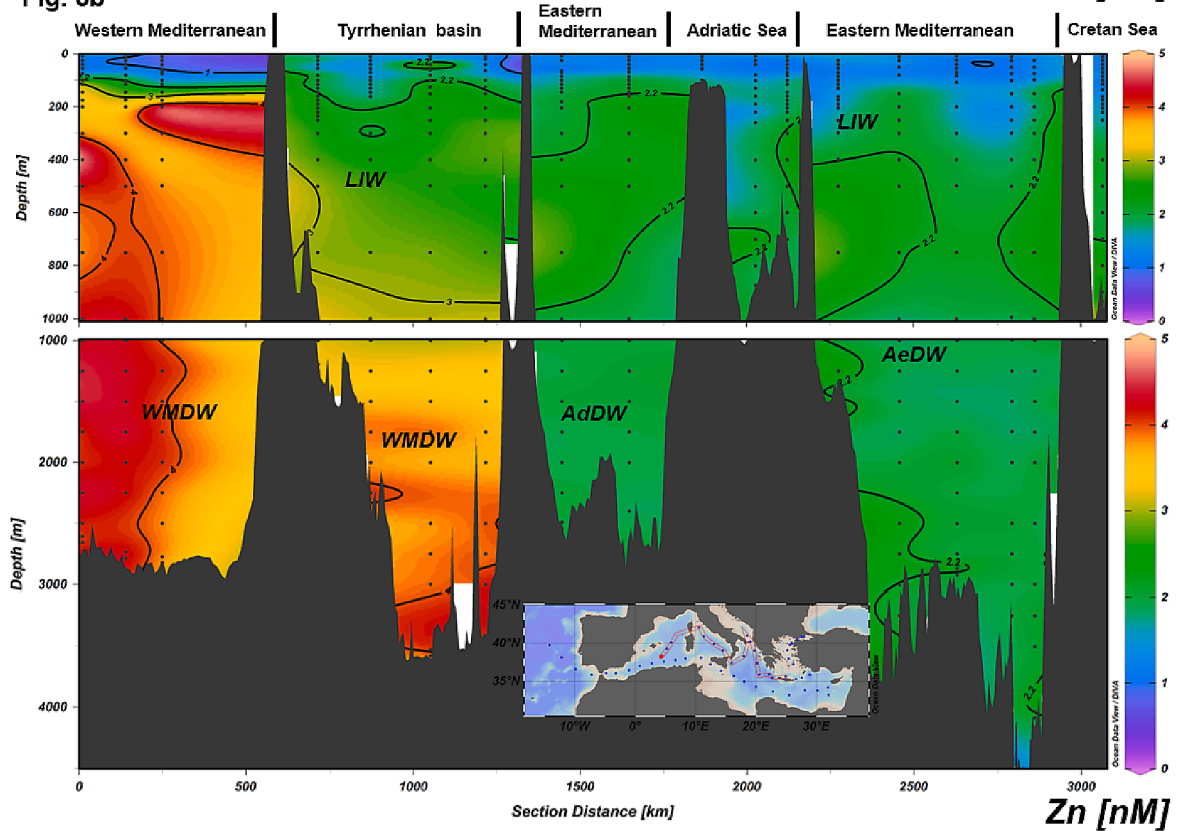
Fig. 5. Distribution of zinc in color scale. 5a Concentration of dissolved Zn (nM) along the Southern transect in the upper 1000 m (upper panel) and the remainder of the water column (lower panel). 5b Concentration of dissolved Zn (nM) along the northern transect in the upper 1000 m (upper panel) and the remainder of the water column (lower panel). Abbreviations as in Fig. 2.
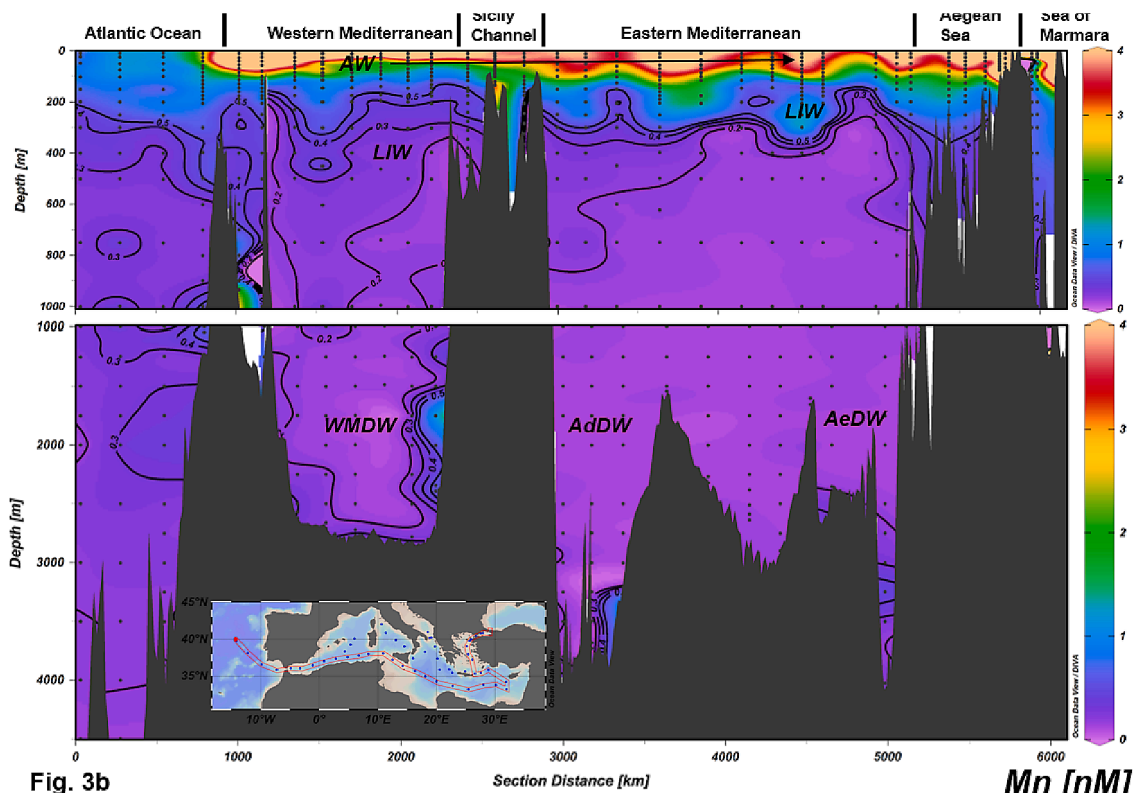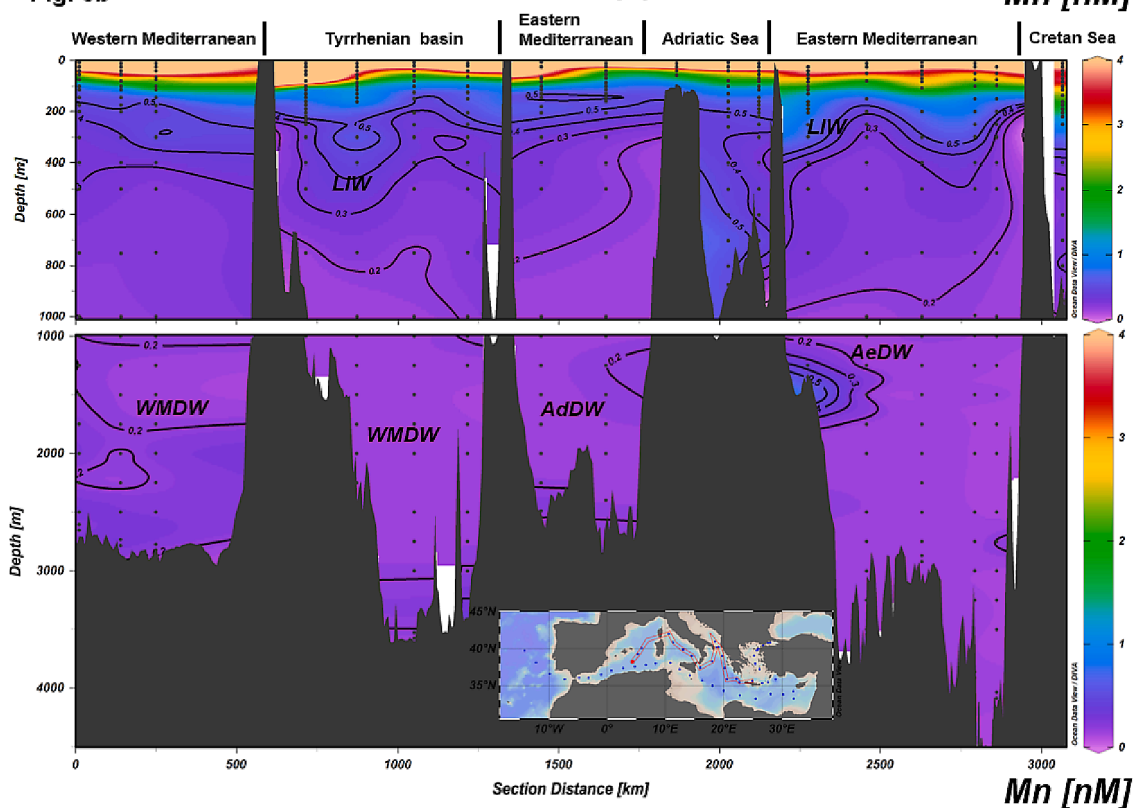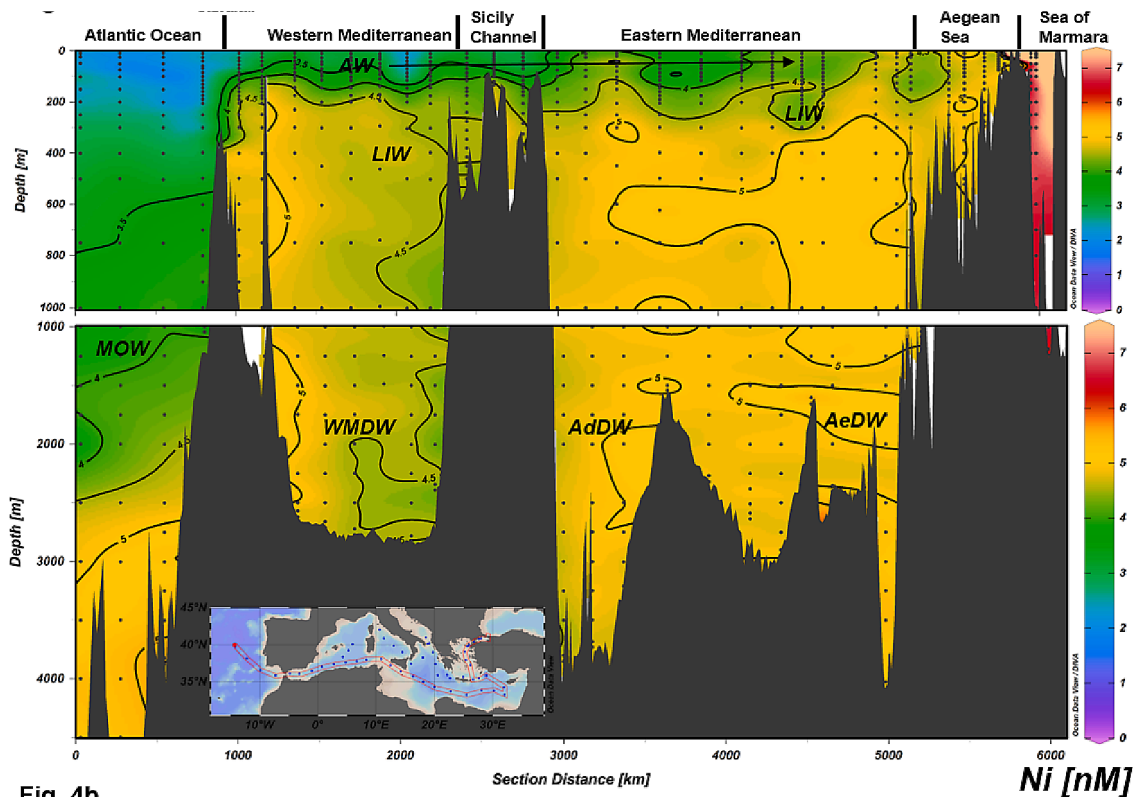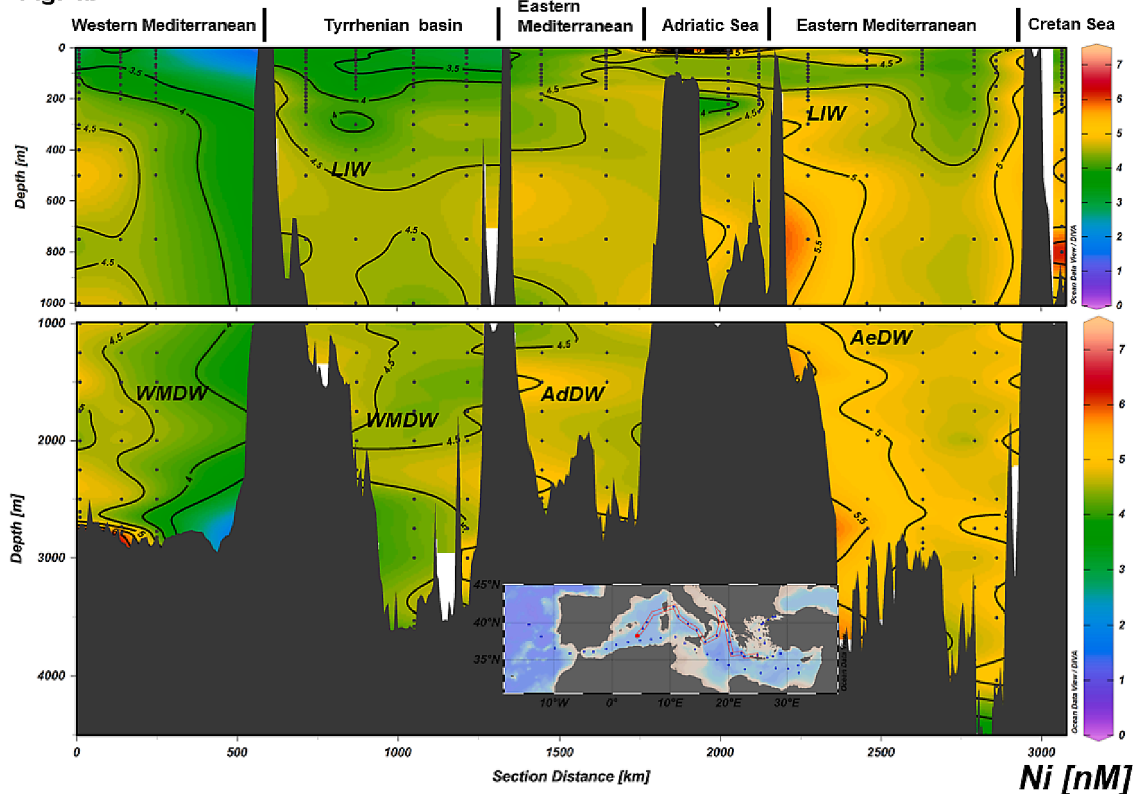
Fig. 6. Distribution of cadmium in color scale. 6a Concentration of dissolved Cd (pM) along the Southern transect in the upper 1000 m (upper panel) and the remainder of the water column (lower panel). 6b Concentration of dissolved Cd (pM) along the northern transect in the upper 1000 m (upper panel) and the remainder of the water column (lower panel). Abbreviations as in Fig. 2.
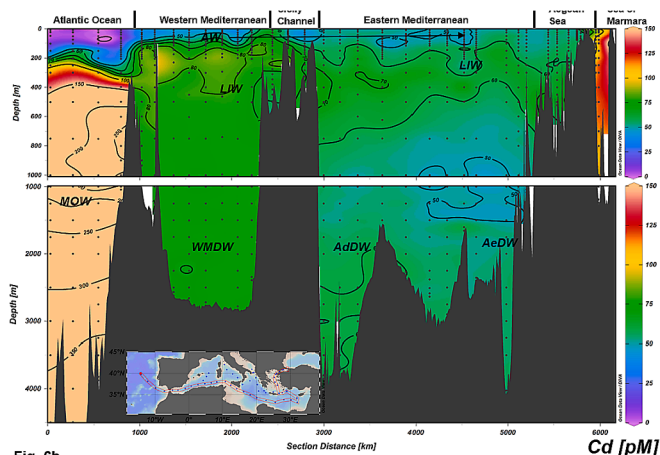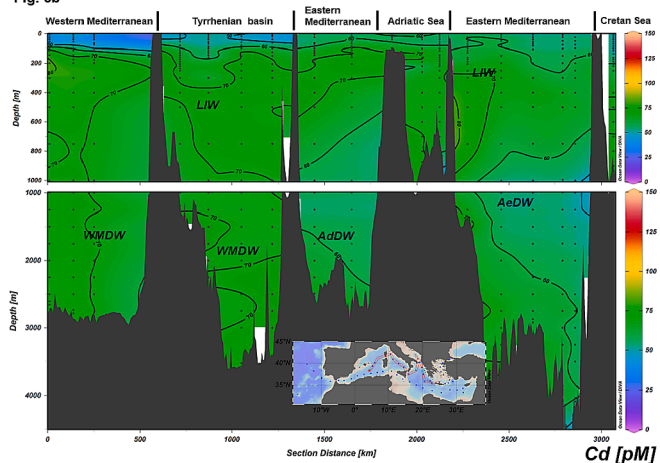
et al., 2014). In the Atlantic Ocean, surface concentrations were between 0.7 and 2.4 nM with the highest concentrations closest to the Strait of Gibraltar (Fig. 3a). In the Mediterranean Sea along the southern transect, surface concentrations were higher than in the Atlantic with concentrations between ~3 and 7 nM, where surface concentrations in the WMED basin were higher (~4–7 nM) than in the EMED basin (~3–4.5 nM). Surface concentrations increased into the Aegean Sea to values >7 nM with the highest concentrations in the Dardanelles (>40 nM) and Sea of Marmara (>30 nM). Along the northern transect, surface concentrations were also somewhat higher in the WMED (~5–7 nM) and Tyrrhenian Sea (~6–8 nM) compared to the EMED (~5–6 nM) with the exception of elevated surface concentrations in the Adriatic Sea (up to 14 nM) (Fig. 3b). With depth, concentrations of Mn decreased rapidly, resulting in concentrations in the range of 1 to 2 nM around 100 m depth, which is elevated compared to the Atlantic, and generally below 0.5 nM deeper than 300 m at which point concentrations in the Mediterranean were generally lower compared to the Atlantic. Deeper than 500 m, especially in AdDW, AeDW and WMDW, dissolved Mn was mostly below 0.2 nM with some sporadic elevations near the seafloor, notably around bathymetric features such as the Strait of Gibraltar or the Channel of Sicily.

3.2.2. Dissolved Ni

Dissolved Ni displayed typical nutrient-like behaviour in the Atlantic Ocean, as is expected in open ocean environments (Bruland et al., 2014). The lowest concentrations of Ni were observed in Atlantic surface water

with concentrations as low as 2 nM and concentrations increased to ~5.5 nM in the deep (Fig. 4a). In the core of MOW, Ni was just below 4 nM. The vertical distribution of Ni in the Mediterranean Sea was quite different than in the Atlantic. In the Mediterranean, the increase in concentrations with depth was steeper than in the Atlantic, but below ~400 m, concentrations were relatively homogenous whereas they continued to increase in the Atlantic. Generally, concentrations of Ni are higher in the Mediterranean than the Atlantic at similar depths. The concentration of Ni was between ~3 and 4.5 nM in surface waters (AW) of the Mediterranean basins and increases to >5 nM in the Adriatic and Aegean Sea. Extremely elevated concentrations of up to 20 nM were observed in the Sea of Marmara. In the deep parts of the EMED and WMED basins, concentrations increased with depth to values that were generally between 4 and 4.5 nM at 200 m depth. In the deep water masses, AdDW, AeDW and WMDW, concentrations were more homogenous with the exception of the deep stations (deeper than 1000 m) near the Aegean (Fig. 4a and b) and Adriatic Sea (Fig. 4b) where concentrations above 5 nM were observed compared to concentrations mostly between 4.5 and 5 nM in the remainder of the Mediterranean basins. Overall, it seems concentrations below 300 m are marginally higher in the EMED (4.91 ± 0.24 nM (1SD)) compared to the WMED (4.58 ± 0.24 nM (1SD)) at stations deeper than 1000 m, but the difference is not resolvable as the averages overlap within 1 SD uncertainty.

3.2.3. Dissolved Zn

Similar to Ni, Zn displayed typical nutrient-like behaviour in the Atlantic Ocean. Minimum Zn concentrations of <0.1 nM were observed in Atlantic surface waters, while concentrations increased to values >3 nM in Atlantic deep waters (Fig. 5a). The concentration of Zn in the core of MOW was ~2 nM. The vertical distribution of Zn in the Mediterranean Sea was strikingly different compared to the Atlantic Ocean with higher concentrations at similar depths in the Mediterranean. The concentration of Zn in the upper 100 m of the WMED water column (AW) was generally just over 1 nM, with the exception of the region south of Sardinia where 2.5 nM was observed. In the EMED, surface concentrations (AW) were similar and concentrations increased towards the Sea of Marmara where values >5 nM were found in the surface and a maximum Zn concentration of 8.3 nM occurred at 100 m depth. Concentrations of Zn increased rapidly with depth (>4 nM at 200 m at a few localities in the WMED), and were homogeneous in WMDW at around 4 nM. In the EMED along the southern transect, the concentration of Zn was ~1 to 1.5 nM in LIW and increased to ~2 to 2.5 nM at depths between ~300 and 750 m. Along the northern transect, surface concentrations in the EMED were similar, but increased to >1.5 around 100 m depth whereas concentrations between ~300 and 750 m were similar (~2 to 2.5 nM) compared to the southern transect (Fig. 5b). The distribution of Zn in AdDW and AeDW ranged between ~1.6 and 2.2 nM, with small patches of >2.2 nM. In general, the concentration of Zn was much higher in the WMED relative to the EMED, especially in intermediate and deep waters with values of 3.9 ± 0.6 nM (1SD) in the WMED and 2.0 ± 0.2 nM (1SD) in the EMED below 300 m for stations deeper than 1000 m depth.

3.2.4. Dissolved Cd

Like Ni and Zn, dissolved Cd displayed nutrient-like behaviour in the Atlantic Ocean. Concentrations of Cd of <10 pM were observed in the upper 100 m, while concentrations steadily increased to values >375 pM in deep waters (Fig. 6a). The concentration of Cd in the core of MOW was ~160 pM closest to the Strait of Gibraltar, which is higher than values in the Mediterranean Sea. The concentration trends of Cd in the Mediterranean were similar to those of Zn. In the WMED, the surface concentrations of Cd were generally around ~35 to 55 pM with slightly higher values south of Sardinia (~70 pM). Concentrations increased to a mid-depth maximum of ~80–90 pM across a depth range of ~150 to 500 m (shallower than the core of LIW), and were more homogeneous at depths deeper than 500 m with concentrations between ~70 and 80 pM. In the EMED, the concentration of Cd in surface waters was ~50 to 60

pM with the highest values in the Adriatic Sea (up to 63 pM). Mid-depth maxima of ~60 to 75 pM were observed across a depth range of ~200 to 450 m within LIW. There was limited variability in the Cd concentrations in AdDW and AeDW below 1000 m with concentrations of ~50 to 65 pM (Fig. 6a and b). Again, similar to Zn, the concentration of Cd was generally elevated in deep waters in the WMED relative to EMED deep waters with values of 59 ± 6 pM (1SD) in the EMED and 73 ± 4 pM (1SD) in the WMED below 300 m for stations deeper than 1000 m depth. Elevated surface and deep concentrations of Cd were observed in the Sea of Marmara with concentrations of up to 120 pM at the mid depth maximum around 400 m depth.

3.2.5. Macro nutrients and oxygen

The trends in the distributions of the macro nutrients (Fig. 7) are similar to the trends observed for the metals with known nutrient type behaviour, Ni, Zn and Cd, although the concentrations of metals were not depleted to very low values in the surface waters of the Mediterranean. Macro nutrients were depleted in the surface layer, most notably in the EMED where depleted concentrations ($PO_4 < 0.1$ µmol/kg; $NO_3 < 1$ µmol/kg and $Si < 2$ µmol/kg) extended to greater depth (~200 m) than in the WMED (~100 m). Concentrations of NO_3 (Fig. 7a) and PO_4 (Fig. 7b) were elevated in deep waters (below 300 m at station deeper than 1000 m depth) in the WMED relative to the EMED with PO_4 and NO_3 concentrations of 0.18 ± 0.04 and 4.84 ± 1 µmol/kg (1SD) in the EMED and 0.38 ± 0.05 and 8.3 ± 0.9 µmol/kg (1SD) in the WMED, respectively. In contrast, no coinciding change in the Si (Fig. 7c) and oxygen concentrations or the apparent oxygen utilization (AOU (derived using ODV version 5.3.0 (Schlitzer, 2020)); Fig. 7d) was observed between the deep basins with respective concentrations in the EMED and WMED of 188.7 ± 7.7 and 185.5 ± 8.5 µmol/kg for oxygen, 7.12 ± 1.9 and 8.05 ± 1.3 µmol/kg for Si, and 60 ± 9 and 66 ± 8 µmol/kg for AOU.

3.3. Flux and budget calculations

The water budget of the Mediterranean is dominated by the fluxes at the Strait of Gibraltar and the Sicily Channel that are on the order of ~1 Sverdrup (Sv) into and out of the basin. There is a small net inflow of Atlantic water compared to the flux of MOW exiting the WMED, resulting in a net exchange of <0.1 Sv into the Mediterranean (Soto-Navarro et al., 2010; Tsimplis et al., 2006). Fluxes of similar magnitude are estimated at the Sicily Channel such that modified AW exits the WMED at the Sicily Channel towards the EMED at a rate of ~1 Sv, and LIW flows in the reverse direction at a similar rate (Van Cappellen et al., 2014). Here we have taken the water cycle model of Powley et al. (2016)

and simplified it by ignoring the net evaporation (i.e. no fluxes out into the atmosphere) as this outward water flux leaves the dissolved metals behind (Fig. 8) and we ignored the limited exchange with the Black Sea. Additionally, we ignored the specific regions of deep-water formation as we do not have estimates for the concentrations of metals in these regions for the time of formation. Moreover, it is an irregular process, complicating quantification. In the simple model, deep water formation happens continuously and fluxes are based on concentrations observed in the stratified summer season. At the Strait of Gibraltar, the metal concentrations in inflowing AW are estimated from the average concentrations in samples from the upper 150 m at station S.4 and the remaining concentrations are estimated as the average observations in the deep basin (using only stations deeper than 1000 m) for the regions and water layers as shown in Fig. 8. This allows the calculation of apparent fluxes for the dissolved metals (Table 3). This model suggests that there is a net flux out of the WMED for all metals, and thus additional sources are needed to balance the budget. For the EMED, there is also an apparent net flux out of the basin of Ni, Zn and Cd whereas there is an apparent net flux of Mn into the basin, requiring a loss term to balance the budget for Mn (Table 3).

4. Discussion

The flux calculations based on the simplified water cycle model after Powley et al. (2016) primarily illustrate that the bio-active metals Mn, Ni, Zn and Cd do not behave conservatively. A conservative mixing model such as this one assumes conservative behaviour and thus no partitioning from the dissolved phase to the particulate phase and vice versa, i.e. ignoring biogeochemical processes such as biological uptake, scavenging and dissolution. Moreover, in this model there is no representation of fluvial or atmospheric input as there are no reliable estimates of the effective dissolved fluxes, i.e. no data on the amount that ends up in solution (dissolved) in the waters of the deep basins due to fluvial or atmospheric input. This model thus indicates where additional input (e.g. atmospheric deposition) or output (e.g. biological uptake) of dissolved metals is required to explain the observations. The fluxes estimated for the WMED are comparable to previous estimates in summer with current estimates constituting between 27 and 93% for Mn, 116 and 174% for Ni, 6 and 96% for Zn and 27 and 109% for Cd, of previously estimated fluxes (Elbaz-Poulichet et al., 2001b; Elbaz-Poulichet et al., 2001c). However for Zn, current estimates are lower than previous estimates for fluxes into the WMED at the Strait of Gibraltar, implying current lower Zn fluxes (see Section 4.2), but inadvertent contamination of pre-GEOTRACES sampling efforts cannot be ruled out either.

As mentioned, the actual concentrations and fluxes are not only governed by water mixing, but importantly, also by removal processes

Fig. 7. Distributions of macro nutrients in color scale. 7a Concentration of dissolved NO_3 (µmol/kg) along the southern transect over the entire water column. 7b Concentration of dissolved PO_4 (µmol/kg) along the southern transect over the entire water column. 7c Concentration of dissolved Si (µmol/kg) along the southern transect over the entire water column. 7d AOU (µmol/kg) along the southern transect over the entire water column. Abbreviations as in Fig. 2.

Fig. 8. Simplified conceptual water cycle model after Powley et al. (2016). This model ignores the net evaporation and input from rivers. Fluxes are in Sv (10^6 m^3 s^{-1}).

Table 3

Fluxes of dissolved metals in the stratified summer season of 2013 calculated based on a simplified water cycle model after Powley et al. (2016) as shown in Fig. 8. A negative (−) flux denotes a flux out of a water mass or basin. Fluxes for metals are shown in Mega mol per year (Mmol/yr), Sv represents the flux of water in 10^6 m^3 s^{-1}.

Upper water West (0–150 m)	Sv	Mn	Ni	Zn	Cd
Strait of Gibraltar	0.83	40.8	58.2	6.9	0.4
Western intermediate water	0.55	7.6	76.8	58.1	1.3
Strait of Sicily	−1.14	−104.9	−124.5	−68.7	−2.0
Western deep water	−0.23	−21.2	−25.1	−13.9	−0.4
Net fluxes	**0.01**	**−77.7**	**−14.6**	**−17.6**	**−0.7**

Intermediate water West (150–600 m)	Sv	Mn	Ni	Zn	Cd
Eastern intermediate water	1.10	12.5	166.1	71.0	2.2
Western deep water	0.37	2.8	53.5	47.5	0.8
Strait of Gibraltar	−0.47	−6.5	−65.6	−49.6	−1.1
Western deep water	−0.45	−6.2	−62.8	−47.5	−1.1
Western upper water	−0.55	−7.6	−76.8	−58.1	−1.3
Net fluxes	**0.00**	**−4.9**	**14.4**	**−36.6**	**−0.4**

Deep water West (>600 m)	Sv	Mn	Ni	Zn	Cd
Western intermediate water i	0.45	6.2	62.8	47.5	1.1
Western upper water	0.23	21.2	25.1	13.9	0.4
Strait of Gibraltar	−0.31	−2.4	−44.9	−39.8	−0.7
Western intermediate water	−0.37	−2.8	−53.5	−47.5	−0.8
Net fluxes	**0.00**	**22.2**	**−10.4**	**−26.0**	**−0.1**

Upper water East (0–200 m)	Sv	Mn	Ni	Zn	Cd
Strait of Sicily	1.14	104.9	124.5	68.7	2.0
Eastern intermediate water	0.02	0.2	3.0	1.3	0.0
Eastern intermediate water	−1.10	−84.9	−148.9	−47.0	−2.1
Net fluxes	**0.06**	**20.2**	**−21.4**	**22.9**	**0.0**

Intermediate water East (200–500 m)	Sv	Mn	Ni	Zn	Cd
Eastern upper water	1.10	84.9	148.9	47.0	2.1
Eastern deep water	0.36	2.0	56.1	22.4	0.7
Western intermediate water	−1.10	−12.5	−166.1	−71.0	−2.2
Eastern deep water	−0.36	−4.1	−54.4	−23.2	−0.7
Net fluxes	**0.00**	**70.3**	**−15.4**	**−24.8**	**−0.3**

Deep water East (>500 m)	Sv	Mn	Ni	Zn	Cd
Eastern intermediate water	0.36	4.1	54.4	23.2	0.7
Eastern intermediate water	−0.36	−2.0	−56.1	−22.4	−0.7
Net fluxes	**0.00**	**2.1**	**−1.7**	**0.9**	**0.1**

and input sources. For the surface WMED, indeed the net negative fluxes estimated with the mixing model (Table 3), demonstrate there is a substantial additional input needed to balance the budget. In comparison, for the surface EMED, a net negative flux is estimated for Ni only, while Cd seems balanced, and for Zn and Mn net export is suggested. This implies that the additional input and removal terms that are present (e.g. dust deposition and biological uptake) are in balance for Cd, whereas for Ni there must be additional input that is sufficient to also compensate for biological removal and any scavenging. For dissolved Zn and Mn, mixing supplies an excess of metals and thus removal processes must dominate over input processes to balance the budget. The residence times of the water masses in the Mediterranean below the upper water layer (Fig. 8) are shorter than the residence times of the metals in the deep ocean, with the exception of Mn (Bruland et al., 2014; Landing and Bruland, 1987), therefore model estimates based on the assumption of conservative behaviour might be more accurate for dissolved Ni, Zn and Cd in the deep, but this is not the case for Mn. Indeed, the net large positive fluxes of Mn into the deep basins imply that mixing supplies an excess of Mn to the deep ocean and a loss term, most likely scavenging

(van Hulten et al., 2017), is needed to balance the budget. In contrast, for Ni, Zn and Cd additional input is needed to balance the budget, notably for Zn and Cd in the deep WMED as discussed in Section 4.2.1.

4.1. Surface distribution

Sources of metals to the upper ocean include continental runoff, atmospheric deposition, submarine groundwater discharge and upwelling of, or mixing with deeper water. The influence of continental runoff and groundwater discharge is expected to be strongest in the coastal zone and an assessment of available data on the metal concentrations in rivers draining into the Mediterranean Sea suggests rivers are a minor source of metals to this oceanic region, relative to sources from atmospheric deposition and inflowing AW at the Strait of Gibraltar (Elbaz-Poulichet, 2005; Elbaz-Poulichet et al., 2001b), whereas no data is available for groundwater discharge (Rodellas et al., 2015).

Within the Mediterranean, our simple model suggests an additional source of metals is needed to balance the budget for surface waters (WMED and EMED combined), with the exception of Zn (Table 3). Given that this model ignores biological uptake and scavenging, the actual required input to balance the budget is in fact even larger. Moreover, given that underlying LIW as well as the deeper Mediterranean water masses are sourced from Mediterranean surface waters, and surface concentrations for all metals discussed here are elevated in Mediterranean compared to Atlantic surface water, an external source of metals is required to explain these high surface concentrations. There is inherent uncertainty in the calculated fluxes (Table 3), but small changes in either the fluxes of water at the straits or changes in the concentrations of dissolved metals in the different water masses would not change the general observation that the physical circulation results in a net negative surface flux (i.e. unbalanced budget) of dissolved metals. However, these calculations based on the open Atlantic Ocean as an endmember might not account for the possible influence of the Tinto–Odiel river system.

The Tinto–Odiel river system in southern Spain that drains into the Atlantic Ocean in the vicinity of the Strait of Gibraltar is a significant source of trace metals, of which the influence varies with seasonal changes in discharge that should have been relatively high during the time of sampling (Elbaz-Poulichet et al., 2001a; Elbaz-Poulichet et al., 2001b; Elbaz-Poulichet et al., 2001c). Surface concentrations of all metals increase from station S3 to S4, located just west of the Strait, implying a role for discharge of this river system as a source of metals to the Mediterranean. Previously it was estimated that riverine discharge could increase the fluxes into the Mediterranean, relative to unaffected AW alone, by a factor of 2.4, 3, and 7, for Cd, Zn and Mn respectively, whereas the effect for Ni was negligible (Elbaz-Poulichet et al., 2001c). When comparing the concentrations of stations S1–S3 to the stations in the WMED in the upper 25 m, the concentrations increase by a factor of ~5, 1.5, 7 and 12, respectively for Mn, Ni, Zn and Cd. Based on the current data it indeed seems likely that the Tinto–Odiel river system is an important source of metals to the inflowing AW, however, given the spatial sampling resolution and positioning of our stations, it is not feasible to unravel the relative contribution of this source, and our estimates based on a single station close to the Strait of Gibraltar might underestimate the flux of metals associated with the inflow of AW (Table 3). Nevertheless, the westward increasing surface concentrations within the Mediterranean and/or the elevated deep concentrations compared to the Atlantic, imply an additional source within the Mediterranean is needed.

Particulate metals, notably labile particulate metals could potentially contribute to the dissolved pool after water masses enter the WMED. Such an effect is difficult to constrain as particulate data are not available for this expedition. Particulate concentrations are usually elevated in the surface and decrease with depth and thus Atlantic surface waters possibly contain elevated concentrations of trace metals in the particulate phase due to biological uptake and atmospheric deposition

(Twining et al., 2015) or local fluvial discharge (Elbaz-Poulichet et al., 2001c). As Atlantic surface water circulates through the Mediterranean Sea, particulate trace metals originating from the Atlantic could be released to the dissolved phase thereby contributing to the flux of trace metals through the straits. Twining et al. (2015) reported levels of labile particulate Ni, Zn, and Cd from Atlantic surface waters off the coast of Portugal determined as part of the 2010/2011 U.S. GEOTRACES North Atlantic Zone Transect. The labile fractions of particulate trace metals were on average less than ~0.25 nM Mn, 40 pM Ni, 0.25 nM Zn and 4 pM Cd, in the upper 150 m. Thus, fluxes of particulate Mn, Ni, Zn and Cd, in the absence of strong riverine sources of particulate metals that are subject to long range transport, are not likely to influence the net flux of trace metals across the Strait of Gibraltar or change the general observation that the distributions of dissolved Ni, Zn and Cd in the Mediterranean Sea require sources of these metals to surface water within the Mediterranean region as well as a local source of Zn and Cd to deep waters in the WMED (see Section 4.2).

Previously it was shown that surface water concentrations of Al increased from west to east due to mixing of low Al Atlantic surface waters with high Al Mediterranean surface and intermediate waters and the enhanced concentrations of Al in Mediterranean waters were attributed to dust deposition (Guerzoni et al., 1999; Rolison et al., 2015). Similar to Al, surface concentrations increase along the eastward flow path of AW for Ni and Cd (Figs. 4a and 6a), but not for Zn or Mn (Figs. 5a and 3a). Such a zonal increase for Ni and Cd was recently also reported by (Tovar-Sánchez et al., 2020), with the highest concentrations occurring in the sea surface microlayer. Most likely, the increasing concentrations partly arise from mixing with underlying waters, but also input of dust, as the primary source of metals to surface waters is atmospheric deposition (Elbaz-Poulichet et al., 2001b), especially during times of limited vertical mixing due to strong stratification as during this study. However, this raises the question why the concentrations of Zn and Mn do not increase along the AW flow path whereas the concentrations of Ni and Cd do increase. This must be related to a balance between input and removal processes other than mixing of water masses (Table 3). In the case of Zn, both scavenging (Weber et al., 2018) and organic complexation (Baars and Croot, 2011) are known to affect the concentration. In the absence of complexation and particulate data, discussion on the underlying processes remains speculative. Nevertheless, dust deposition not only is a source of metals, it also leads to scavenging (Bressac et al., 2021; Gerringa et al., 2017; Sarthou and Jeandel, 2001; Wagener et al., 2010) presumably through the influx of particulates into the water column, and it is thus plausible that the rather homogenous surface concentration of Zn on the order of 1 to 1.5 nM in the upper ~50 m of the water column (Fig. 5; outside the shallow shelf seas) is the equilibrium concentration resulting from the interplay between dissolution and organic complexation on one hand, and scavenging and biological uptake on the other hand. The fraction of total Zn that is adsorbed onto particles is thought to be small, ~0.5% in the upper ocean (Weber et al., 2018), and thus biological uptake is most likely dominating dissolved Zn removal in the surface layer. This was also suggested based on results for the sea surface microlayer in the same region (Tovar-Sánchez et al., 2020). The concentrations of Ni and Cd are also partly governed by organic complexation (e.g. Baars et al., 2014; Morel et al., 2014), but not known to be strongly affected by scavenging in oxygenated seawater, leading to conservative behaviour in the deep ocean and a residence time that exceeds the time of global ocean circulation (e.g. Middag et al., 2020; Middag et al., 2018). Additionally, Ni has been associated with an inhibiting role on microbial growth in the Mediterranean (Tovar-Sánchez et al., 2020). The combination of a small influence of scavenging and limited biological uptake in one of the most oligotrophic seas in the world, supposedly allows the concentrations of Ni and Cd to build up in Mediterranean surface waters. The more oligotrophic conditions in the EMED compared to the WMED (Pujo-Pay et al., 2011), probably contribute to the observed west to east gradient in metal concentrations. In contrast, Mn has a much shorter residence time

and is prone to oxidative scavenging (Landing and Bruland, 1980) which can be microbially mediated (Sunda and Huntsman, 1988). The dynamics between dust input and reductive dissolution on one hand and scavenging and uptake on the other hand apparently lead to a far more 'patchy' distribution in Mediterranean surface water than observed for the other metals discussed here, similar to observations for iron (Gerringa et al., 2017). Overall, the surface distributions of metals in the Mediterranean are a testament to the dynamics of their biogeochemical cycling. Fast cycling between the dissolved and particulate pools leads to a patchier distribution for elements like Mn, whereas elements like Ni and Cd with a longer residence time accumulate in AW while it advects east, despite net losses estimated based on conservative mixing.

4.1.1. Atmospheric deposition

Atmospheric deposition in the Mediterranean Sea is a source of metals with variable anthropogenic and natural origins (Guieu et al., 2010; Migon and Caccia, 1990) and likely a crucial factor in closing the budget for the surface ocean (Table 3). The natural dust deposition from the Saharan desert to the Mediterranean as well as to the Atlantic basin, all the way to the Amazon rain forest, is well known as it is tracked using satellite data (e.g. Yu et al., 2015). However, as detailed in the introduction, anthropogenic sources too play an important role in the Mediterranean. The natural lithogenic contribution to atmospheric deposition of metals to surface waters can be estimated by analysing the ratio of the metal content to the Al content in the atmospheric aerosol particles themselves and comparison of these ratios to the metal/Al ratios (Me/Al) in the source lithogenic material. Elevated Me/Al ratios in atmospheric particles relative to the background Me/Al ratios in the Saharan dust end member indicate an additional source (i.e. anthropogenic). This normalization method assumes that anthropogenic sources of Al in atmospheric particles are negligible and that Al in atmospheric particles is nearly completely derived from a single lithogenic source with known Me/Al ratios. Using this method, Guieu et al. (2010) estimated that at the scale of the entire Mediterranean Sea the atmospheric deposition of Fe is ~89% lithogenic in origin, while Zn, Cd, and Pb are ~88%, 96%, and 81% anthropogenic in origin, respectively. To the best of our knowledge, no such estimates exist for Ni and Mn at the basin scale. Nevertheless, for atmospheric aerosols at Cap Ferrat (France), in the north-west Mediterranean between 1998 and 2008, Heimbürger et al. (2010) regularly observed enrichment factors >100 for Ni (enrichment factor = $(Ni/Al)_{aerosol}$ / $(Ni/Al)_{lithogenic}$; thus an enrichment factor of 100 implies an anthropogenic fraction of 99%), mostly in autumn and winter, but enrichment factors were variable and values <10 were also found. Given that the crustal abundance of Ni is similar to Zn (Taylor, 1964), that the solubility of dust from North Africa is in the same range for both metals (up to ~40%; Shelley et al. (2018); their figure 5), and that the concentration increase from Atlantic surface water to Mediterranean surface water was also similar, one would expect the anthropogenic contribution for Ni to be roughly be the same order of magnitude as Zn when assuming similar residence times. However, Heimbürger et al. (2010) classified Ni as a trace metal with an intermediate anthropogenic contribution for which the anthropogenic contribution is not as dominant as for Zn and Cd for which they found even higher enrichment factors than for Ni. Therefore, here we also assume the anthropogenic contribution for Ni is intermediate and falls between the contributions of Fe on one hand, and Zn and Cd on the other hand. For Mn, the crustal abundance is more than an order of magnitude lower than for Fe (5.6 vs 0.1% (Taylor, 1964)), but Mn solubility from dust is much higher compared to Fe (<10% for Fe and up to 60% for Mn; Shelley et al. (2018); their figure 5). Heimbürger et al. (2010) reported anthropogenic fractions <80% for Mn in aerosols, which was higher than anthropogenic fractions for Fe. Therefore, the elevated concentrations of Mn in the surface Mediterranean could be due lithogenic dust deposition with a small anthropogenic contribution, but the influence of the Tinto–Odiel river system on the inflowing AW likely also plays a role.

Overall, atmospheric deposition is most likely a primary source of

metals within the Mediterranean where Zn and Cd, and possibly Ni, are suggested to be dominantly derived from anthropogenic sources. This implies that the elevated concentrations of Ni, Zn and Cd in Mediterranean surface and deep waters relative to inflowing AW (Figs. 4a, 5a and 6a) could be a consequence of atmospheric deposition of anthropogenic particles. The elevated concentrations of Zn and Cd in WMED deep waters relative to EMED deep waters (Figs. 5 and 6) and the apparent 'missing' deep water flux (i.e. flux required to balance the budget) (Table 3) may be related to spatial gradients in atmospheric deposition of anthropogenic particles and/or other processes that may redistribute dissolved metals within the confines of the Mediterranean Sea, as discussed below.

4.2. Deep distribution

4.2.1. Interbasin fractionation and the deep WMED

The distributions of dissolved metals in the Mediterranean Sea display striking inter-basin fractionations with elevated concentrations of Zn and Cd in the deep water of the WMED basin compared to the deep EMED basin (Figs. 5 and 6). For Mn, no interbasin difference could be determined (Fig. 3) and Ni concentrations appear marginally higher in the deep EMED (Fig. 4; see Section 3.2). Besides Zn and Cd, also the concentrations of the macro nutrients NO_3 and PO_4 were elevated in the deep WMED relative to the deep EMED whereas this was not the case for Si (Fig. 7a, b and c). Since deep EMED waters contribute to deep WMED waters (see Section 2.3.), the higher PO_4 and NO_3 concentrations in the deep WMED could indicate more (accumulated) remineralization overall in the latter basin. The absence of a coinciding increase of Si would indicate siliceous diatoms do not play a significant role in primary productivity in the Mediterranean, in contrast to previous studies (e.g. Psarra et al., 2000; Rigual-Hernández et al., 2013; Vidussi et al., 2001). Moreover, no coinciding decrease in oxygen concentrations, or increase in AOU was observed (Fig. 7d), clearly indicating that differences in the amount of remineralization are not causing the interbasin fractionation.

This is further illustrated by the regressions between the different elements with interbasin fractionation and AOU (Fig. 9) were the deep EMED waters have lower concentrations at similar AOU compared to the deep WMED. Additionally, the residence time of deep waters in the WMED (~42 years) is shorter than the residence time in the EMED (~150 years) (Powley et al., 2016; Van Cappellen et al., 2014) (Fig. 8), and hence a larger influx into the WMED is required to reach similar deep equilibrium concentrations. This is further underlined by the simple conservative mixing model (Section 3.3) that estimates a net flux of Cd and Zn out of the WMED from the intermediate and deep layers that is a factor 2–3 higher than in the EMED, and thus requiring additional input of Cd and Zn, especially into the WMED. Thus, to explain the differences in the deep concentrations, an additional source of Zn, Cd, PO_4 and NO_3 to the deep WMED is required that would not lead to strong enhancements in the concentrations of Ni and Si.

The distribution trends of Zn and Cd in the WMED are quite similar with both elements displaying lower concentrations in surface waters compared to intermediate and deep waters (Figs. 5 and 6). Upward advection and turbulent mixing between LIW and AW supplies the upper water column with Zn and Cd (Table 3). The high concentrations of Zn and Cd in LIW and WMDW, in turn, must be supported by a source of these metals to intermediate and deep waters in the WMED (Table 3), also considering the higher concentrations in LIW in the WMED relative to LIW in the EMED where this water mass is formed (Figs. 5 and 6). Since atmospheric deposition of anthropogenic particles is considered to be the primary source of Zn and Cd to the Mediterranean Sea (see Section 4.1), there also must be vertical transport of Zn and Cd from surface waters to deep waters, such as deep-water formation or vertical transport via sinking particles. The formation of WMDW primarily occurs in the region of the Gulf of Lions (Millot and Taupier-Letage, 2005), and therefore it is important to constrain the concentrations of dissolved metals in this region in order to better understand how deep water formation controls the dissolved metal concentrations in WMDW as that is not accounted for by our simple conservative mixing model.
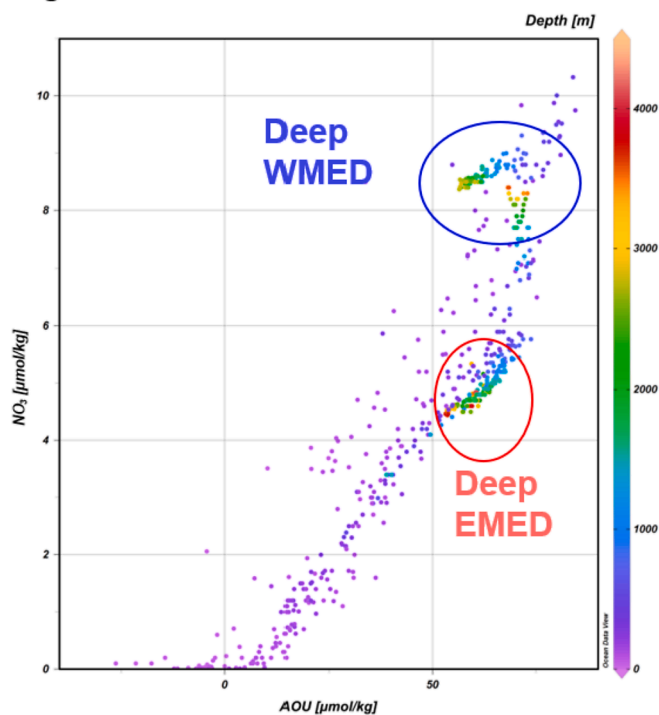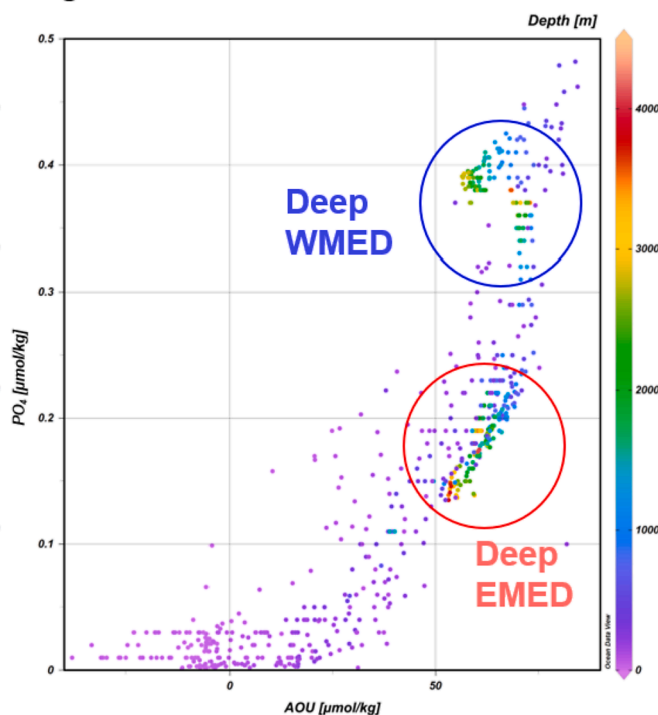

Fig. 9. Macro nutrients versus Apparent Oxygen Ultilization (AOU) along both transects for stations deeper than 1000 m. 9a Concentration of dissolved NO_3 (μmol/kg) versus AOU (μmol/kg). 9b Concentration of dissolved PO_4 (μmol/kg) versus AOU (μmol/kg). 9c Concentration of dissolved Zn (nM) versus AOU (μmol/kg). 9d Concentration of dissolved Cd (pM) versus AOU (μmol/kg).

Unfortunately, no stations were occupied in this region during the 2013 GEOTRACES expeditions, precluding a detailed discussion of the dissolved metal concentrations in WMDW precursor water. To the best of our knowledge, there is no trace metal concentration data available for the Gulf of Lions, but there is the DYFAMED time series station for which seasonal dissolved Ni is available (Migon et al., 2020) as well as one profile for dissolved Cd (Lacan et al., 2006) and this time series station is located to the east of this region, where the prevailing currents should transport waters from the DYFAMED region to the Gulf of Lions (Migon et al., 2020). Concentrations of Ni varied mainly between ~3.5 and 4.5 nM in surface water and between 4.5 and 5 nM in deep water throughout the year at the DYFAMED station (Migon et al., 2020). This is very similar to the range in surface water (~3 to 4.5 nM) as well as the range (4.58 ± 0.24 nM) observed in the current data for the station located in the deep WMED. For dissolved Cd, one profile is available at the same DYFAMED station from summer 2003 with concentrations that ranged between 65 and 69 pM in the upper 50 m, followed by a mid-depth maximum at 100 m depth (88 pM) and ~75 pM in the deep (Lacan et al., 2006). These surface concentrations are slightly higher than most of the current observations (~35 to 55 pM), but similar to values south of Sardinia or in the Adriatic Sea, whereas the mid-depth maximum and deep values are again very similar to the current data for the deep WMED (73 ± 4 pM). Given that there is no indication that Cd and Ni concentrations are strongly elevated in the formation region of WMDW compared to the formation region of EMDW (see Section 4.2.2) and assuming there is no stark contrast for Zn either, there must be an alternative source for the elevated levels of Cd and Zn in the deep WMED. This is also confirmed by the current data in the WMED along the part of the northern transect that traversed the WMED from north to south (station N.17-N.18; Fig. 5b and 6b). There was no increasing trend in the concentrations towards the northern formation region of WMDW, whereas this would be expected if elevated concentrations in the WMDW formation region would be the cause for the higher concentrations in the deep WMED compared to the deep EMED, especially given the recent ventilation event in the Gulf of Lions (in the winter (2012−2013) prior to the current observations (Testor et al., 2018)).

Overall, there is no evidence for a strong signal in the WMDW formation region. Moreover, higher concentrations in the WMDW formation region would also not explain higher concentrations in LIW in the WMED relative to LIW in the EMED where this water mass is formed. This leaves a vertical flux of metal laden particles dissolving through the water column of the WMED, or deep sedimentary input, as a source for the elevated concentrations in the deep basins. This could be related to atmospheric deposition or terrestrial inputs, such as runoff, as most stations occupied along the southern transect are <100 km away from the nearest land mass and can therefore still be influenced by coastal processes (Morley et al., 1997). Despite the generally narrow continental shelves, Katz et al. (2020) demonstrated sediment originating from the continental margins can be transported at least 100 km offshore based on a site in the EMED where at least 60% of the sediment flux that reached the seafloor arrived via lateral transport rather than via particles exported vertically from the upper water column. Assuming this is representative for other locations in the Mediterranean, particulate material deposited on the continental shelfs via run off or atmospheric deposition could also significantly contribute to the particulate trace metal pool of the deep basins and, via partial dissolution either in the water column or at the sediment water interface, also to the dissolved metals pool. Regardless of the exact mechanism of transport to the deep WMED basin, elevated concentrations of Cd and Zn must result from local sources of these metals that are most likely anthropogenic. Based on the simple mixing model, a flux of ~0.5 Mmol yr^{-1} Cd and ~68.7 Mmol yr^{-1} Zn is needed to balance the budget for dissolved metals in the deep WMED, or a flux of ~1.2 Mmol yr^{-1} Cd and ~80.2 Mmol yr^{-1} Zn for the WMED overall. For Cd, the invoked overall missing flux is ~3.5 times the maximum previous estimate of atmospheric flux, whereas for Zn the overall missing flux is ~1.3 times the maximum previous

estimate of atmospheric flux (Elbaz-Poulichet et al., 2001b). Riverine fluxes within the Mediterranean have been estimated to be <12% of atmospheric fluxes (Elbaz-Poulichet et al., 2001b) and are thus unlikely to be relevant (see Section 4.1). Moreover, the relative importance of the Tinto–Odiel river system is greater for Zn than for Cd (Elbaz-Poulichet et al., 2001a; Elbaz-Poulichet et al., 2001c). Thus an overestimation of the invoked flux due to under sampling of this fluvial input outside the Mediterranean, seems an unlikely reason for the large apparent missing flux for Cd as this should have affected the apparent missing Zn flux more strongly. This would suggest increased atmospheric deposition over the last 2 decades based on the apparent missing fluxes (Table 3), notably for Cd. However, time-series measurements show an ~66 and 54% decrease in the Cd and Zn concentrations, respectively, in atmospheric aerosols at Cap Ferrat, France in the north-west Mediterranean between 1998 and 2008 (Heimbürger et al., 2010). If this is a general trend around the Mediterranean, trace metal concentrations of anthropogenically derived metals in Mediterranean waters should decrease with time as well. However, deep water measurements of trace metals are scarce, and comparisons with data preceding the GEOTRACES era might be subject to artefacts as sampling and analytical techniques have improved (Anderson, 2020). Nevertheless, the average concentration of dissolved Zn of 3.9 ± 0.6 nM (1SD) in the WMED below 300 m for stations deeper than 1000 m depth is very similar to the average total (unfiltered) Zn concentration of 4.0 ± 0.5 nM (1SD) at depths deeper than 300 m in the WMED in 1983 as reported by Ruiz-Pino et al. (1991). The similarity of the two estimates suggests that the sources of Zn to the deep WMED have remained relatively constant for at least three decades. Nevertheless, in 1983, much higher surface concentrations (up to ~7 nM) were observed that were attributed to recent anthropogenic sources (Ruiz-Pino et al., 1991). These authors predicted the Zn cycle would come to a steady state some decades after Zn sources to the Mediterranean stabilized, with surface concentrations lower than the deep concentrations, as that is the normal state for a nutrient type element. The current observations of lower surface concentrations seem consistent with this notion and thus might reflect that Zn sources have stabilized since the 1980's, or that the peak in Zn emissions has passed as supported by the observations by Heimbürger et al. (2010). For Cd, current concentrations in WMED below 300 m for stations deeper than 1000 m depth (73 ± 4 pM) are comparable to prior observations for WMDW (77 ± 16 pM) (Morley et al., 1997) whereas current concentrations in the upper 50 m (~46 pM) might be slightly lower than observations in the early 1990s (~60 pM) (Morley et al., 1997) or 1980s (70–90~pM) (Copin-Montegut et al., 1986; Laumond et al., 1984), where importantly, surface concentrations were similar or elevated relative to deep concentrations for the earliest studies. This might imply, akin to argued for Zn, that atmospheric sources of Cd have decreased. Based on the current data, it is impossible to firmly conclude whether there has been an increase or decrease in metal input over the last several decades. Nevertheless, the change in vertical profile shape, i.e. surface concentrations enriched relative to deep concentration compared to currently depleted surface concentrations, is not likely explained by seasonal (Migon et al., 2020) or methodological changes, and thus it is more likely that input of Cd and Zn has decreased.

Summarizing, the anthropogenic origins of Zn and Cd are reflected in higher concentrations in the deep WMED (Figs. 5 and 6). This is not seen for Ni (Fig. 4) that is known to be influenced by a combination of anthropogenic and lithogenic sources and for Mn no stark contrast was observed between the deep EMED and WMED (Fig. 3). For Mn, this is not only related to the largely lithogenic sources, but similar to observations in the surface, are also due to the biogeochemistry of Mn in which scavenging plays an important role (see Section 4.1). The higher concentrations of anthropogenically derived metals in the deep WMED imply anthropogenic emissions to the WMED have exceeded those to the EMED in the last decades, especially given the shorter residence time of WMED waters. Based on the observations for the major nutrients (NO$_3$ and PO$_4$; Fig. 7a and b), the inputs of Zn and Cd are associated with

inputs of NO_3 and PO_4, in agreement with recent studies that also attributed large fractions of atmospheric NO_3 and PO_4 deposition in the Mediterranean to anthropogenic sources (Kanakidou et al., 2020; Pavlidou et al., 2020). Assuming the observed trends at Cap Ferrat in aerosols are representative for the entire Mediterranean region, emissions for Zn and Cd have decreased. If the decreasing trend in surface concentrations of Zn and Cd between the 1980s and 2013 is indeed representative despite different sampling and analytical techniques, this would confirm this trend of decreasing emissions and imply past emissions have found their way into the deep WMED and/or sediments and might have exited via the Strait of Gibraltar with MOW. However, to confirm such a trend or detect others, regular basin wide assessments of the trace metal distributions in the Mediterranean are needed.

4.2.2. Deep EMED

The distribution trends of Ni, Zn and Cd resembled each other in the EMED, as in the WMED, and display maximum concentrations over a broad depth range of ~200 to 750 m (Figs. 4, 5 and 6). Within this depth range there are two intermediate water masses. The intermediate water masses formed in the EMED in the largest volume and with the highest salinity is LIW. The CIW, which forms in the Cretan Sea, a sub-basin of the southern Aegean Sea, forms with a slightly greater density than LIW and therefore resides below LIW in the water column (Velaoras et al., 2014). As LIW has a higher salinity than CIW, the maximum concentrations observed across the depth range of ~200 to 750 m should correlate with the highest salinities if the maxima originate in LIW. However, maximum concentrations across this depth range did not correlate with the highest salinities (and therefore LIW), but rather correlate with a denser, less saline water mass deeper in the water column. The maximum concentrations clustered around a potential density anomaly (σ) between ~29.10 and 29.17 kg/m^3 which is within the range of the observed σ of CIW (29.1 to 29.2 kg/m^3) produced between 2007 and 2009 (Velaoras et al., 2014). Station N.1 is the only station from the 2013 GEOTRACES expedition located within the Cretan Sea (Fig. 1). Elevated concentrations of Ni, Zn and Cd were observed in deep waters at station N.1 (Figs. 4b, 5b and 6b), and support the role of CIW as the source of elevated Ni, Zn and Cd concentrations observed in the EMED across a depth range of ~200 to 750 m. Interestingly, the concentrations of Ni, Zn and Cd in AeDW, which also partly forms in the Cretan Sea, are not noticeably elevated (Figs. 4, 5 and 6) implying different water masses are utilized during intermediate versus deep water formation or temporal differences in the dissolved metal content in dense water forming within the Cretan basin.

4.3. Atlantic and MOW

The bio-active metals all displayed typical open ocean profiles at the four stations in the Atlantic Ocean where Ni, Cd and Zn (Figs. 4a, 5a and 6a) are depleted in the surface ocean due to biological uptake and concentrations increase with depth due to remineralisation (e.g. Bruland et al., 2014). The profile of Mn (Fig. 3a) is different as the distribution of Mn is not significantly influenced by biological uptake outside the Southern Ocean (e.g. Middag et al., 2011) and is mainly driven by (atmospheric) input and photo reduction in the surface layer and scavenging in the deep (e.g. van Hulten et al., 2017 and references therein). The general Atlantic distributions of dissolved Ni, Cd, Zn and Mn have been described in detail elsewhere (e.g. Conway and John, 2014; Conway and John, 2015; Hatta et al., 2015; Middag et al., 2018, 2019, 2020; Roshan and Wu, 2015a, 2015b; van Hulten et al., 2017) and are not further discussed. However, the data presented here are well suited to assess the influence of the MOW on the distribution of metals in the Atlantic. The MOW contains preformed metal concentrations that differ from the adjacently located water masses present in the Atlantic Ocean and thus can lead to elevated concentrations of metals in the Atlantic as previously shown for e.g. dissolved Al (Measures et al., 2015; Rolison et al., 2015) and Pb (Rusiecka et al., 2018) or particulate Fe (Thuróczy

et al., 2010). Specifically, there is net export of dissolved Zn into the Atlantic (Table 3) and the concentrations of Zn are elevated relative to water masses residing shallower and deeper than MOW in the water column of the Atlantic Ocean (Fig. 5a) and hence MOW leads to an elevation of Zn in the Atlantic Ocean around 1250 m as observed previously (Conway and John, 2014). In the case of dissolved Ni, there is also net export into the Atlantic (Table 3) and the concentrations are higher in the Mediterranean than the Atlantic (Fig. 4a). But unlike for Zn, MOW does not appear as a distinct mid-depth concentration maximum for Ni as the underlying water in the Atlantic has similar Ni concentrations. Despite the net export of dissolved Cd into the Atlantic (Table 3), the concentration of Cd was lower in MOW than the overlying and underlying water (Fig. 6a), and the presence of MOW indeed results in a Cd minimum in the Atlantic Ocean as reported previously (Conway and John, 2015). The concentration of Cd in the core of MOW near the strait of Gibraltar (~160 pM) was higher than observed values in the Mediterranean Sea, indicating significant mixing between MOW and Atlantic waters has occurred. The concentration minimum in MOW despite net export of Cd into the Atlantic results from the relatively deep position of MOW in the Atlantic (core around 1250 m) as a consequence of its density and the presence of relatively Cd-rich water masses shallower and deeper in the Atlantic. The concentrations of Mn in the central deep Mediterranean basins appear slightly lower than at similar depth in the Atlantic Ocean (Fig. 3a). However, Mn concentrations in MOW appear as a mid-depth concentration maximum for Mn with concentrations around 0.3 nM and up to 0.6 nM near the strait of Gibraltar. Thus even though concentrations are elevated in the MOW, this Mn is not sourced from the Mediterranean waters, but most likely results from interaction of MOW with the sediments as sediments are a known source of Mn due to reductive dissolution or sediment resuspension (e.g. van Hulten et al., 2017 and references therein). Based on the simple conservative mixing model, MOW is a source of Ni, Cd and Zn, and the influence of MOW leads to distinct features in the distributions of metals in the Atlantic Ocean for Mn, Zn and Cd, whereas the influence for Ni is more subtle.

4.4. Sea of Marmara

The Sea of Marmara receives inflow of Black Sea surface water via the Bosporus Strait whereas deep waters are mainly supplied from inflow of dense Mediterranean water via the Dardanelles (Beşiktepe et al., 1994). Surface concentrations of Mn, Ni, Zn and Cd in the Sea of Marmara were all elevated relative to surface concentrations observed elsewhere in the Mediterranean (Figs. 3a, 4a, 5a and 6a). Inflow of relatively fresh Black Sea surface water via the shallow Bosporus cannot be the only source of these surface elevations as surface concentrations in the Black Sea were lower than in the Sea of Marmara (Rolison, 2016). Nevertheless, surface concentrations of Ni and Mn were significantly correlated to salinity in the upper 25 m of the water column ($p < 0.05$) with the highest concentrations corresponding to the lowest salinities. For Cd, the regression was not significant ($p = 0.18$) and for Zn no trend was observed, implying that mixing between Black Sea surface water and Mediterranean water was not a strong control on the upper water column distribution for the latter two metals. The steep halocline present in the Sea of Marmara prevents efficient overturning of deep water which results in the consumption of dissolved oxygen (<50 μmol/kg below ~100 m) due to aerobic respiration of sinking particulate organic matter whose production in surface waters is supported by runoff of nutrients from anthropogenic sources in the region (Beşiktepe et al., 1994; Çolpan Polat and Tugrul, 1995). The latter runoff apparently also supplies Mn, Ni, Zn and Cd given the higher surface concentrations relative to surface concentrations elsewhere in the Mediterranean (Figs. 3a, 4a, 5a and 6a). Scavenging onto sinking particles is an important control on the distributions of Mn and possibly Zn in the open ocean. Especially Mn concentrations decreased markedly from values >30 nM near the Sea of Marmara surface to <1 nM below the oxycline

with enrichments near the sediments (up to ~10 nM; Fig. 3a). Overall, concentrations of Mn were higher compared to concentrations in the Mediterranean basins. Concentrations of Zn increased with depth to a maximum (>8 nM) just below the oxycline (Fig. 5a). Deeper concentrations remained high to a depth of ~300 m, followed by a decrease with depth to values around 3 nM. This was higher than concentrations at similar depth in the EMED, but lower compared to the WMED. Under low oxygen conditions, preservation of particulate organic matter is increased due to low respiration rates which should act to enhance scavenging efficiency. This could potentially explain the decrease in Zn as well as Mn concentrations, as usually elevated Mn concentrations are observed in low oxygen zones in the open ocean, notably near the sediments (e.g. Hatta et al., 2015; van Hulten et al., 2017). In the Sea of Marmara, elevated concentrations were observed near the sediment (up to ~10 nM), illustrating there is supply of Mn from sediments under low oxygen conditions, but supply from either the surface or the sediments does not persist in the water column here (Fig. 3a), and scavenging is the most likely explanation for this distribution of Mn below the surface layer. The distribution of Zn apparently is less sensitive to scavenging as concentrations are elevated at depths were Mn was already depleted. At these depths (~100–300 m depth) there was a dynamic interplay by supply via remineralization and removal via scavenging and we postulate that supply dominates over removal for Zn in this depth range and scavenging removal dominates deeper than ~300 m, whereas for Mn scavenging removal dominates already below ~100 m depth. In the case of Cd, the distribution was more similar to Zn than Mn, with a subsurface maximum (Fig. 6a). However, this maximum of ~120 pM was located deeper, around 400 m, compared to the Zn maximum just below the oxycline. Deeper than this maximum, concentrations of Cd decrease slightly but remain elevated compared to the Mediterranean with values generally ~110 pM. We postulate this distribution results from Cd being slightly susceptible to scavenging, but even less than Zn, leading to supply from remineralization dominating till greater depth. Additionally, the low metal concentrations (cf. surface waters) in the deepest part of this enclosed basin could also be related to inflow of dense Mediterranean water with lower concentrations via the Dardanelles. Nevertheless, the absence of a subsurface Mn maximum and the differing depths of the subsurface maxima for Cd and Zn do invoke a role for scavenging that affects Mn the most, and Cd the least of these 3 metals if one assumes no differences in depth of remineralization between these metals. Concentrations of Ni sharply decrease from extremely elevated surface concentrations (up to 20 nM) to values around 7 nM below the oxycline due to mixing with the underlying relatively Ni poor water, with slightly lower values around 6.5 nM in the deepest parts (Fig. 4a). The distribution of Ni below the oxycline suggests that out of Mn, Ni, Zn and Cd, Ni is least affected by scavenging and a limited role for scavenging was also suggested for the Mediterranean basin (see Section 4.1). Overall, the distributions of Mn, Ni, Zn and Cd in the Sea of Marmara illustrate all of these metals can be affected by surface sources, most likely of anthropogenic origin given the urban surroundings of this sea, as previously suggested for nutrients (Çolpan Polat and Tugrul, 1995), and intensive marine traffic. In the presence of such a strong source, the different susceptibilities of the dissolved metals distributions to supply from remineralization and removal through scavenging is even more apparent than in the Mediterranean basins.

5. Conclusions

As demonstrated previously for other metals, the distribution of bio-active metals Mn, Ni, Zn and Cd in the Mediterranean Sea is also heavily influenced by dust deposition, leading to elevated surface concentrations compared to the Atlantic Ocean. Given that Mediterranean deep waters are sourced from local surface waters, the outflow of Mediterranean water into the Atlantic leads to a net flux of Ni, Zn and Cd to the Atlantic Ocean. However, as Mn is sensitive to scavenging removal, elevated Mn concentrations in MOW are not the result of elevated

concentrations in the deep Mediterranean basin, but most likely the result of interaction with the sediments around the Strait of Gibraltar. In contrast to Mn, the concentrations of Zn and Ni were elevated relative to concentrations at similar depth in the Atlantic Ocean, especially for Zn in the WMED. Despite concentrations of Cd generally being lower in the deep Mediterranean compared to similar depths in the Atlantic Ocean, the increase in concentrations with increasing depth was steeper in the Mediterranean in the upper water column (~200 m), especially in the WMED. For all four metals, additional sources to inflow from the Atlantic Ocean are needed to explain the observed distributions, especially in the WMED for Cd and Zn. The WMED apparently is more affected by anthropogenic sources, notably for Zn and Cd, but not as strongly as the Sea of Marmara. Tentative comparisons with historic data suggest that anthropogenic emissions of Zn and Cd into the WMED might have peaked and that deep concentrations should decrease in the coming decades, but this remains speculative. Anthropogenic input of Cd and Zn likely results from a combination of direct atmospheric inputs, but transport of shelf derived material into the deep basins cannot be excluded either. The distribution of Mn in the deep basins is mainly governed by its biogeochemistry, especially scavenging removal, whereas lithogenic and anthropogenic influences are restricted to the surface waters with some influence of sediment sources in the deep basin. Scavenging removal also seems to play a role for the distribution of Zn in the Mediterranean, as inferred previously for the global distribution, especially in the Pacific (Weber et al., 2018), whereas the effects are not obvious in the Atlantic (Middag et al., 2019; Weber et al., 2018). For Cd, scavenging removal plays a small role that was mainly apparent in the heavily anthropogenically impacted Sea of Marmara whereas for Ni scavenging removal was not obvious. The deep distribution of Ni is likely also affected by anthropogenic sources, but given that the deep concentrations are not elevated in the deep WMED relative to the deep EMED, the internal biogeochemical cycling and lithogenic sources play a more important role than anthropogenic deposition. Overall, this basin wide dataset from the GEOTRACES project underlines that the Mediterranean Sea is susceptible to anthropogenic disturbances where the consequences for the distributions of bio-active metals depend on the source strength as well as their respective biogeochemical cycles. Close monitoring of the Mediterranean Sea is needed to evaluate changing anthropogenic influences on regional biogeochemical cycles and this study provides a first baseline to asses future changes.

References

Alonso Castillo, M.L., Sánchez Trujillo, I., Vereda Alonso, E., García de Torres, A., Cano Pavón, J.M., 2013. Bioavailability of heavy metals in water and sediments from a typical Mediterranean Bay (Málaga Bay, Region of Andalucía, Southern Spain). Mar. Pollut. Bull. 76 (1), 427–434.

Anderson, R.F., 2020. GEOTRACES: accelerating research on the marine biogeochemical cycles of trace elements and their isotopes. Annu. Rev. Mar. Sci. 12 (1), 49–85.

Baars, O., Croot, P.L., 2011. The speciation of dissolved zinc in the Atlantic sector of the Southern Ocean. Deep-Sea Res. II Top. Stud. Oceanogr. 58 (25), 2720–2732.

Baars, O., Abouchami, W., Galer, S.J.G., Boye, M., Croot, P.L., 2014. Dissolved cadmium in the Southern Ocean: distribution, speciation, and relation to phosphate. Limnol. Oceanogr. 59 (2), 385–399.

Benedicto, J., Andral, B., Martínez-Gómez, C., Guitart, C., Deudero, S., Cento, A., Scarpato, A., Caixach, J., Benbrahim, S., Chouba, L., Boulahdid, M., Galgani, F., 2011. A large scale survey of trace metal levels in coastal waters of the Western Mediterranean basin using caged mussels (Mytilus galloprovincialis). J. Environ. Monit. 13 (5), 1495–1505.

Beşiktepe, Ş.T., Sur, H.İ., Özsoy, E., Latif, M.A., Oğuz, T., Ünlüata, Ü., 1994. The circulation and hydrography of the Marmara Sea. Prog. Oceanogr. 34 (4), 285–334.

Biller, D.V., Bruland, K.W., 2012. Analysis of Mn, Fe, Co, Ni, Cu, Zn, Cd, and Pb in seawater using the Nobias-chelate PA1 resin and magnetic sector inductively coupled plasma mass spectrometry (ICP-MS). Mar. Chem. 130–131 (0), 12–20.

Boyle, E.A., Chapnick, S.D., Bai, X.X., Spivack, A., 1985. Trace metal enrichments in the Mediterranean Sea. Earth Planet. Sci. Lett. 74 (4), 405–419.

Bressac, M., Wagener, T., Leblond, N., Tovar-Sánchez, A., Ridame, C., Albani, S., Guasco, S., Dufour, A., Jacquet, S., Dulac, F., Desboeufs, K., Guieu, C., 2021. Subsurface iron accumulation and rapid aluminium removal in the Mediterranean following African dust deposition. Biogeosci. Discuss. 2021, 1–29.

Bruland, K.W., Middag, R., Lohan, M.C., 2014. 8.2 - controls of trace metals in seawater A2 - Holland, Heinrich D. In: Turekian, K.K. (Ed.), Treatise on Geochemistry (Second Edition). Elsevier, Oxford, pp. 19–51.

Çolpan Polat, S., Tugrul, S., 1995. Nutrient and organic carbon exchanges between the Black and Marmara seas through the Bosphorus Strait. Cont. Shelf Res. 15 (9), 1115–1132.

Conway, T.M., John, S.G., 2014. The biogeochemical cycling of zinc and zinc isotopes in the North Atlantic Ocean. Glob. Biogeochem. Cycles 28 (10), 2014GB004862.

Conway, T.M., John, S.G., 2015. Biogeochemical cycling of cadmium isotopes along a high-resolution section through the North Atlantic Ocean. Geochim. Cosmochim. Acta 148 (0), 269–283.

Copat, C., Bella, F., Castaing, M., Fallico, R., Sciacca, S., Ferrante, M., 2012. Heavy metals concentrations in fish from Sicily (Mediterranean Sea) and evaluation of possible health risks to consumers. Bull. Environ. Contam. Toxicol. 88 (1), 78–83.

Copin-Montegut, G., Courau, P., Nicolas, E., 1986. Distribution and transfer of trace elements in the Western Mediterranean. Mar. Chem. 18 (2), 189–195.

Cossa, D., Buscail, R., Puig, P., Chiffoleau, J.F., Radakovitch, O., Jeanty, G., Heussner, S., 2014. Origin and accumulation of trace elements in sediments of the northwestern Mediterranean margin. Chem. Geol. 380, 61–73.

De Baar, H.J.W., Timmermans, K.R., Laan, P., De Porto, H.H., Ober, S., Blom, J.J., Bakker, M.C., Schilling, J., Sarthou, G., Smit, M.G., Klunder, M., 2008. Titan: a new facility for ultraclean sampling of trace elements and isotopes in the deep oceans in the international Geotraces program. Mar. Chem. 111 (1–2), 4–21.

Dulaquais, G., Planquette, H., L'Helguen, S., Rijkenberg, M.J.A., Boye, M., 2017. The biogeochemistry of cobalt in the Mediterranean Sea. Glob. Biogeochem. Cycles 31 (2), 377–399.

Dumas, C., Ludwig, W., Aubert, D., Eyrolle, F., Raimbault, P., Gueneugues, A., Sotin, C., 2015. Riverine transfer of anthropogenic and natural trace metals to the Gulf of lions (NW Mediterranean Sea). Appl. Geochem. 58, 14–25.

Durrieu de Madron, X., Guieu, C., Sempéré, R., Conan, P., Cossa, D., D'Ortenzio, F., Estournel, C., Gazeau, F., Rabouille, C., Stemmann, L., Bonnet, S., Diaz, F., Koubbi, P., Radakovitch, O., Babin, M., Baklouti, M., Bancon-Montigny, C., Belviso, S., Bensoussan, N., Bonsang, B., Bouloubassi, I., Brunet, C., Cadiou, J.F., Carlotti, F., Chami, M., Charmasson, S., Charrière, B., Dachs, J., Doxaran, D., Dutay, J.C., Elbaz-Poulichet, F., Eléaume, M., Eyrolles, F., Fernandez, C., Fowler, S., Francour, P., Gaertner, J.C., Galzin, R., Gasparini, S., Ghiglione, J.F., Gonzalez, J.L., Goyet, C., Guidi, L., Guizien, K., Heimbürger, L.E., Jacquet, S.H.M., Jeffrey, W.H., Joux, F., Le Hir, P., Leblanc, K., Lefèvre, D., Lejeusne, C., Lemé, R., Loÿe-Pilot, M.D., Mallet, M., Méjanelle, L., Mélin, F., Mellon, C., Mérigot, B., Merle, P.L., Migon, C., Miller, W.L., Mortier, L., Mostajir, B., Mousseau, L., Moutin, T., Para, J., Pérez, T., Petrenko, A., Poggiale, J.C., Prieur, L., Pujo-Pay, M., Pulido, V., Raimbault, P., Rees, A.P., Ridame, C., Rontani, J.F., Ruiz Pino, D., Sicre, M.A., Taillandier, V., Tamburini, C., Tanaka, T., Taupier-Letage, I., Tedetti, M., Testor, P., Thébault, H., Thouvenin, B., Touratier, F., Tronczynski, J., Ulses, C., Van Wambeke, F., Vantrepotte, V., Vaz, S., Verney, R., 2011. Marine ecosystems' responses to climatic and anthropogenic forcings in the Mediterranean. Prog. Oceanogr. 91 (2), 97–166.

Elbaz-Poulichet, F., 2005. River inputs of metals and arsenic. In: Saliot, A. (Ed.), The Mediterranean Sea. Springer, Berlin Heidelberg, Berlin, Heidelberg, pp. 211–235.

Elbaz-Poulichet, F., Braungardt, C., Achterberg, E., Morley, N., Cossa, D., Beckers, J.-M., Nomérange, F., Cruzado, A., Leblanc, M., 2001a. Metal biogeochemistry in the Tinto–Odiel rivers (Southern Spain) and in the Gulf of Cadiz: a synthesis of the results of TOROS project. Cont. Shelf Res. 21 (18), 1961–1973.

Elbaz-Poulichet, F., Guieu, C., Morley, N.H., 2001b. A reassessment of trace metal budgets in the Western Mediterranean Sea. Mar. Pollut. Bull. 42 (8), 623–627.

Elbaz-Poulichet, F., Morley, N.H., Beckers, J.-M., Nomerange, P., 2001c. Metal fluxes through the strait of Gibraltar: the influence of the Tinto and Odiel rivers (SW Spain). Mar. Chem. 73 (3), 193–213.

Gerringa, L.J.A., Slagter, H.A., Bown, J., van Haren, H., Laan, P., de Baar, H.J.W., Rijkenberg, M.J.A., 2017. Dissolved Fe and Fe-binding organic ligands in the Mediterranean Sea – GEOTRACES G04. Mar. Chem. 194, 100–113.

Grasshoff, K., Erhardt, M., Kremling, K., 1983. Methods in Seawater Analyses. Verlag Chemie, Weinheim, Germany.

Guerzoni, S., Chester, R., Dulac, F., Herut, B., Loÿe-Pilot, M.-D., Measures, C., Migon, C., Molinaroli, E., Moulin, C., Rossini, P., Saydam, C., Soudine, A., Ziveri, P., 1999. The role of atmospheric deposition in the biogeochemistry of the Mediterranean Sea. Prog. Oceanogr. 44 (1), 147–190.

Guieu, C., Chester, R., Nimmo, M., Martin, J.M., Guerzoni, S., Nicolas, E., Mateu, J., Keyse, S., 1997. Atmospheric input of dissolved and particulate metals to the northwestern Mediterranean. Deep-Sea Res. II Top. Stud. Oceanogr. 44 (3), 655–674.

Guieu, C., Loÿe-Pilot, M.D., Benyahya, L., Dufour, A., 2010. Spatial variability of atmospheric fluxes of metals (Al, Fe, Cd, Zn and Pb) and phosphorus over the whole Mediterranean from a one-year monitoring experiment: biogeochemical implications. Mar. Chem. 120 (1), 164–178.

Hatta, M., Measures, C.I., Wu, J., Roshan, S., Fitzsimmons, J.N., Sedwick, P., Morton, P., 2015. An overview of dissolved Fe and Mn distributions during the 2010–2011 U.S. GEOTRACES north Atlantic cruises: GEOTRACES GA03. Deep-Sea Res. II Top. Stud. Oceanogr. 116 (0), 117–129.

Heimbürger, L.-E., Migon, C., Dufour, A., Chiffoleau, J.-F., Cossa, D., 2010. Trace metal concentrations in the North-western Mediterranean atmospheric aerosol between 1986 and 2008: seasonal patterns and decadal trends. Sci. Total Environ. 408 (13), 2629–2638.

Jordi, A., Basterretxea, G., Tovar-Sánchez, A., Alastuey, A., Querol, X., 2012. Copper aerosols inhibit phytoplankton growth in the Mediterranean Sea. Proc. Natl. Acad. Sci. 109 (52), 21246.

Kanakidou, M., Myriokefalitakis, S., Tsagkaraki, M., 2020. Atmospheric inputs of nutrients to the Mediterranean Sea. Deep-Sea Res. II Top. Stud. Oceanogr. 171, 104606.

Kassis, D., Korres, G., 2020. Hydrography of the Eastern Mediterranean basin derived from argo floats profile data. Deep-Sea Res. II Top. Stud. Oceanogr. 171, 104712.

Katz, T., Weinstein, Y., Alkalay, R., Biton, E., Toledo, Y., Lazar, A., Zlatkin, O., Soffer, R., Rahav, E., Sisma-Ventura, G., Bar, T., Ozer, T., Gildor, H., Almogi-Labin, A., Kanari, M., Berman-Frank, I., Herut, B., 2020. The first deep-sea mooring station in the eastern Levantine basin (DeepLev), outline and insights into regional sedimentological processes. Deep-Sea Res. II Top. Stud. Oceanogr. 171, 104663.

Lacan, F., Francois, R., Ji, Y., Sherrell, R.M., 2006. Cadmium isotopic composition in the ocean. Geochim. Cosmochim. Acta 70 (20), 5104–5118.

Landing, W.M., Bruland, K.W., 1980. Manganese in the North Pacific. Earth Planet. Sci. Lett. 49 (1), 45–56.

Landing, W.M., Bruland, K.W., 1987. The contrasting biogeochemistry of iron and manganese in the Pacific-Ocean. Geochim. Cosmochim. Acta 51 (1), 29–43.

Laumond, F., Copin-Montegut, G., Courau, P., Nicolas, E., 1984. Cadmium, copper and lead in the western Mediterranean Sea. Mar. Chem. 15 (3), 251–261.

Martín, J., Sanchez-Cabeza, J.A., Eriksson, M., Levy, I., Miquel, J.C., 2009. Recent accumulation of trace metals in sediments at the DYFAMED site (northwestern Mediterranean Sea). Mar. Pollut. Bull. 59 (4), 146–153.

Measures, C., Hatta, M., Fitzsimmons, J., Morton, P., 2015. Dissolved Al in the zonal N Atlantic section of the US GEOTRACES 2010/2011 cruises and the importance of hydrothermal inputs. Deep-Sea Res. II Top. Stud. Oceanogr. 116, 176–186.

Middag, R., de Baar, H.J.W., Laan, P., Cai, P.H., van Ooijen, J., 2011. Dissolved manganese in the Atlantic sector of the Southern Ocean. Deep-Sea Research Part Ii-Topical Studies in Oceanography 58 (25–26), 2661–2677.

Middag, R., Séférian, R., Conway, T.M., John, S.G., Bruland, K.W., de Baar, H.J.W., 2015. Intercomparison of dissolved trace elements at the Bermuda Atlantic Time Series station. Marine Chemistry 177 (Part 3), 476–489.

Middag, R., van Heuven, S.M.A.C., Bruland, K.W., de Baar, H.J.W., 2018. The relationship between cadmium and phosphate in the Atlantic Ocean unravelled. Earth Planet. Sci. Lett. 492, 79–88.

Middag, R., de Baar, H.J.W., Bruland, K.W., 2019. The relationships between dissolved zinc and major nutrients phosphate and silicate along the GEOTRACES GA02 transect in the West Atlantic Ocean. Glob. Biogeochem. Cycles 33 (1), 63–84.

Middag, R., de Baar, H.J.W., van Heuven, S.M.A.C., 2020. The distribution of nickel in the West-Atlantic Ocean, its relationship with phosphate and a comparison to cadmium and zinc. Front. Mar. Sci. 7 (105).

Migon, C., Caccia, J.-L., 1990. Separation of anthropogenic and natural emissions of particulate heavy metals in the western Mediterranean atmosphere. Atmos. Environ. Part A 24 (2), 399–405.

Migon, C., Heimbürger-Boavida, L.-E., Dufour, A., Chiffoleau, J.-F., Cossa, D., 2020. Temporal variability of dissolved trace metals at the DYFAMED time-series station. Northwestern Mediterranean. Marine Chemistry 225, 103846.

Millot, C., Taupier-Letage, I., 2005. Circulation in the Mediterranean Sea. In: Saliot, A. (Ed.), The Mediterranean Sea. Springer, Berlin Heidelberg, Berlin, Heidelberg, pp. 29–66.

Moore, C.M., Mills, M.M., Arrigo, K.R., Berman-Frank, I., Bopp, L., Boyd, P.W., Galbraith, E.D., Geider, R.J., Guieu, C., Jaccard, S.L., Jickells, T.D., La Roche, J., Lenton, T.M., Mahowald, N.M., Maranon, E., Marinov, I., Moore, J.K., Nakatsuka, T., Oschlies, A., Saito, M.A., Thingstad, T.F., Tsuda, A., Ulloa, O., 2013. Processes and patterns of oceanic nutrient limitation. Nat. Geosci. 6 (9), 701–710.

Morel, F.M.M., Milligan, A.J., Saito, M.A., 2014. 8.5 - marine bioinorganic chemistry: the role of trace metals in the oceanic cycles of major nutrients. In: Holland, H.D., Turekian, K.K. (Eds.), Treatise on Geochemistry, Second edition. Elsevier, Oxford, pp. 123–150.

Morley, N.H., Burton, J.D., Tankere, S.P.C., Martin, J.M., 1997. Distribution and behaviour of some dissolved trace metals in the western Mediterranean Sea. Deep-Sea Res. II Top. Stud. Oceanogr. 44 (3), 675–691.

Nicolau, R., Lucas, Y., Merdy, P., Raynaud, M., 2012. Base flow and stormwater net fluxes of carbon and trace metals to the Mediterranean Sea by an urbanized small river. Water Resos. 46 (20), 6625–6637.

Nieto, J.M., Sarmiento, A.M., Olías, M., Canovas, C.R., Riba, I., Kalman, J., Delvalls, T.A., 2007. Acid mine drainage pollution in the Tinto and Odiel rivers (Iberian Pyrite Belt, SW Spain) and bioavailability of the transported metals to the Huelva estuary. Environ. Int. 33 (4), 445–455.

Oursel, B., Garnier, C., Durrieu, G., Mounier, S., Omanović, D., Lucas, Y., 2013. Dynamics and fates of trace metals chronically input in a Mediterranean coastal zone impacted by a large urban area. Mar. Pollut. Bull. 69 (1), 137–149.

Pavlidou, A., Velaoras, D., Karageorgis, A.P., Rousselaki, E., Parinos, C., Dähnke, K., Möbius, J., Meador, T.B., Psarra, S., Frangoulis, C., Souvermezoglou, E., Androni, A., Assimakopoulou, G., Chaikalis, S., Kanellopoulos, T.D., Lagaria, A., Zachioti, P., Gogou, A., 2020. Seasonal variations of biochemical and optical properties, physical dynamics and N stable isotopic composition in three northeastern Mediterranean basins (Aegean, Cretan and Ionian seas). Deep-Sea Res. II Top. Stud. Oceanogr. 171, 104704.

Powley, H.R., Krom, M.D., Van Cappellen, P., 2016. Circulation and oxygen cycling in the Mediterranean Sea: sensitivity to future climate change. Journal of Geophysical Research: Oceans 121 (11), 8230–8247.

Psarra, S., Tselepides, A., Ignatiades, L., 2000. Primary productivity in the oligotrophic Cretan Sea (NE Mediterranean): seasonal and interannual variability. Prog. Oceanogr. 46 (2), 187–204.

Pujo-Pay, M., Conan, P., Oriol, L., Cornet-Barthaux, V., Falco, C., Ghiglione, J.F., Goyet, C., Moutin, T., Prieur, L., 2011. Integrated survey of elemental stoichiometry (C, N, P) from the western to eastern Mediterranean Sea. Biogeosciences 8 (4), 883–899.

Rigual-Hernández, A.S., Bárcena, M.A., Jordan, R.W., Sierro, F.J., Flores, J.A., Meier, K.J. S., Beaufort, L., Heussner, S., 2013. Diatom fluxes in the NW Mediterranean: evidence from a 12-year sediment trap record and surficial sediments. J. Plankton Res. 35 (5), 1109–1125.

Rijkenberg, M.J.A., de Baar, H.J.W., Bakker, K., Gerringa, L.J.A., Keijzer, E., Laan, M., Laan, P., Middag, R., Ober, S., van Ooijen, J., Ossebaar, S., van Weerlee, E.M., Smit, M.G., 2015. "PRISTINE", a new high volume sampler for ultraclean sampling of trace metals and isotopes. Marine Chemistry 177 (Part 3), 501–509.

Rodellas, V., Garcia-Orellana, J., Masqué, P., Feldman, M., Weinstein, Y., 2015. Submarine groundwater discharge as a major source of nutrients to the Mediterranean Sea. Proc. Natl. Acad. Sci. 112 (13), 3926.

Rolison, J.M., 2016. The Biogeochemistry of Trace Metals and their Isotopes in the Mediterranean and Black Seas. Thesis, Doctor of Philosophy Thesis. University of Otago. http://hdl.handle.net/10523/6395.

Rolison, J.M., Middag, R., Stirling, C.H., Rijkenberg, M.J.A., de Baar, H.J.W., 2015. Zonal distribution of dissolved aluminium in the Mediterranean Sea. Marine Chemistry 177 (Part 1), 87–100.

Roshan, S., Wu, J., 2015a. Cadmium regeneration within the North Atlantic. Glob. Biogeochem. Cycles 29 (12), 2082–2094.

Roshan, S., Wu, J., 2015b. Water mass mixing: the dominant control on the zinc distribution in the North Atlantic Ocean. Glob. Biogeochem. Cycles 29 (7), 1060–1074.

Ruiz-Pino, D.P., Nicolas, E., Béthoux, J.P., Lambert, C.E., 1991. Zinc budget in the Mediterranean Sea: a hypothesis for non-steady-state behavior. Mar. Chem. 33 (1), 145–169.

Rusiecka, D., Gledhill, M., Milne, A., Achterberg, E.P., Annett, A.L., Atkinson, S., Birchill, A., Karstensen, J., Lohan, M., Mariez, C., Middag, R., Rolison, J.M., Tanhua, T., Ussher, S., Connelly, D., 2018. Anthropogenic signatures of Lead in the Northeast Atlantic. Geophys. Res. Lett. 45 (6), 2734–2743.

Sarthou, G., Jeandel, C., 2001. Seasonal variations of iron concentrations in the Ligurian Sea and iron budget in the Western Mediterranean Sea. Mar. Chem. 74 (2), 115–129.

Schlitzer, R., 2020. Ocean Data View. https://odv.awi.de.

Schlitzer, R., Anderson, R.F., Dodas, E.M., Lohan, M., Geibert, W., Tagliabue, A., Bowie, A., Jeandel, C., Maldonado, M.T., Landing, W.M., Cockwell, D., Abadie, C., Abouchami, W., Achterberg, E.P., Agather, A., Aguliar-Islas, A., van Aken, H.M., Andersen, M., Archer, C., Auro, M., de Baar, H.J., Baars, O., Baker, A.R., Bakker, K., Basak, C., Baskaran, M., Bates, N.R., Bauch, D., van Beek, P., Behrens, M.K., Black, E., Bluhm, K., Bopp, L., Bouman, H., Bowman, K., Bown, J., Boyd, P., Boye, M., Boyle, E.A., Branellec, P., Bridgestock, L., Brissebrat, G., Browning, T., Bruland, K.W., Brumsack, H.-J., Brzezinski, M., Buck, C.S., Buck, K.N., Buesseler, K., Bull, A., Butler, E., Cai, P., Mor, P.C., Cardinal, D., Carlson, C., Carrasco, G., Casacuberta, N., Casciotti, K.L., Castrillejo, M., Chamizo, E., Chance, R., Charette, M. A., Chaves, J.E., Cheng, H., Chever, F., Christl, M., Church, T.M., Closset, I., Colman, A., Conway, T.M., Cossa, D., Croot, P., Cullen, J.T., Cutter, G.A., Daniels, C., Dehairs, F., Deng, F., Dieu, H.T., Duggan, B., Dulaquais, G., Dumousseaud, C., Echegoyen-Sanz, Y., Edwards, R.L., Ellwood, M., Fahrbach, E., Fitzsimmons, J.N., Russell Flegal, A., Fleisher, M.Q., van de Flierdt, T., Frank, M., Friedrich, J., Fripiat, F., Frölje, H., Galer, S.J.G., Gamo, T., Ganeshram, R.S., Garcia-Orellana, J., Garcia-Solsona, E., Gault-Ringold, M., George, E., Gerringa, L.J.A., Gilbert, M., Godoy, J.M., Goldstein, S.L., Gonzalez, S.R., Grissom, K., Hammerschmidt, C., Hartman, A., Hassler, C.S., Hathorne, E.C., Hatta, M., Hawco, N., Hayes, C.T., Heimbürger, L.-E., Helgoe, J., Heller, M., Henderson, G.M., Henderson, P.B., van Heuven, S., Ho, P., Horner, T.J., Hsieh, Y.-T., Huang, K.-F., Humphreys, M.P., Isshiki, K., Jacquot, J.E., Janssen, D.J., Jenkins, W.J., John, S., Jones, E.M., Jones, J. L., Kadko, D.C., Kayser, R., Kenna, T.C., Khondoker, R., Kim, T., Kipp, L., Klar, J.K., Klunder, M., Kretschmer, S., Kumamoto, Y., Laan, P., Labatut, M., Lacan, F., Lam, P.

J., Lambelet, M., Lamborg, C.H., Le Moigne, F.A.C., Le Roy, E., Lechtenfeld, O.J., Lee, J.-M., Lherminier, P., Little, S., López-Lora, M., Lu, Y., Masque, P., Mawji, E., McClain, C.R., Measures, C., Mehic, S., Barraqueta, J.-L.M., van der Merwe, P., Middag, R., Mieruch, S., Milne, A., Minami, T., Moffett, J.W., Moncoiffe, G., Moore, W.S., Morris, P.J., Morton, P.L., Nakaguchi, Y., Nakayama, N., Niedermiller, J., Nishioka, J., Nishiuchi, A., Noble, A., Obata, H., Ober, S., Ohnemus, D.C., van Ooijen, J., O'Sullivan, J., Owens, S., Pahnke, K., Paul, M., Pavia, F., Pena, L.D., Peters, B., Planchon, F., Planquette, H., Pradoux, C., Puigcorbé, V., Quay, P., Queroue, F., Radic, A., Rauschenberg, S., Rehkämper, M., Rember, R., Remenyi, T., Resing, J.A., Rickli, J., Rigaud, S., Rijkenberg, M.J.A., Rintoul, S., Robinson, L.F., Roca-Martí, M., Rodellas, V., Roeske, T., Rolison, J.M., Rosenberg, M., Roshan, S., Rutgers van der Loeff, M.M., Ryabenko, E., Saito, M.A., Salt, L.A., Sanial, V., Sarthou, G., Schallenberg, C., Schauer, U., Scher, H., Schlosser, C., Schnetger, B., Scott, P., Sedwick, P.N., Semiletov, I., Shelley, R., Sherrell, R.M., Shiller, A.M., Sigman, D.M., Singh, S.K., Slagter, H.A., Slater, E., Smethie, W.M., Snaith, H., Sohrin, Y., Sohst, B., Sonke, J.E., Speich, S., Steinfeldt, R., Stewart, G., Stichel, T., Stirling, C.H., Stutsman, J., Swarr, G.J., Swift, J.H., Thomas, A., Thorne, K., Till, C.P., Till, R., Townsend, A.T., Townsend, E., Tuerena, R., Twining, B.S., Vance, D., Velazquez, S., Venchiarutti, C., Villa-Alfageme, M., Vivancos, S.M., Voelker, A.H.L., Wake, B., Warner, M.J., Watson, R., van Weerlee, E., Alexandra Weigand, M., Weinstein, Y., Weiss, D., Wisotzki, A., Woodward, E.M.S., Wu, J., Wu, Y., Wuttig, K., Wyatt, N., Xiang, Y., Xie, R.C., Xue, Z., Yoshikawa, H., Zhang, J., Zhang, P., Zhao, Y., Zheng, L., Zheng, X.-Y., Zieringer, M., Zimmer, L.A., Ziveri, P., Zunino, P., Zurbrick, C., 2018. The GEOTRACES intermediate data product 2017. Chem. Geol. 493, 210–223.

Shelley, R.U., Landing, W.M., Ussher, S.J., Planquette, H., Sarthou, G., 2018. Regional trends in the fractional solubility of Fe and other metals from North Atlantic aerosols (GEOTRACES cruises GA01 and GA03) following a two-stage leach. Biogeosciences 15 (8), 2271–2288.

Skliris, N., 2014. Past, present and future patterns of the thermohaline circulation and characteristic water masses of the Mediterranean Sea. In: Goffredo, S., Dubinsky, Z. (Eds.), The Mediterranean Sea: Its History and Present Challenges. Springer, Netherlands, Dordrecht, pp. 29–48.

Soto-Navarro, J., Criado-Aldeanueva, F., García-Lafuente, J., Sánchez-Román, A., 2010. Estimation of the Atlantic inflow through the Strait of Gibraltar from climatological and in situ data. Journal of Geophysical Research: Oceans 115 (C10).

Statham, P.J., Burton, J.D., Hydes, D.J., 1985. Cd and Mn in the Alboran Sea and adjacent North Atlantic: geochemical implications for the Mediterranean. Nature 313 (6003), 565–567.

Sunda, W.G., Huntsman, S.A., 1988. Effect of sunlight on the redox cycles of manganese in the southwestern Sargasso Sea. Deep-Sea Research Part a-Oceanographic Research Papers 35 (8), 1297–1317.

Taylor, S.R., 1964. Abundance of chemical elements in the continental crust: a new table. Geochim. Cosmochim. Acta 28 (8), 1273–1285.

Testor, P., Bosse, A., Houpert, L., Margirier, F., Mortier, L., Legoff, H., Dausse, D., Labaste, M., Karstensen, J., Hayes, D., Olita, A., Ribotti, A., Schroeder, K., Chiggiato, J., Onken, R., Heslop, E., Mourre, B., D'ortenzio, F., Mayot, N., Lavigne, H., de Fommervault, O., Coppola, L., Prieur, L., Taillandier, V., Durrieu de Madron, X., Bourrin, F., Many, G., Damien, P., Estournel, C., Marsaleix, P., Taupier-Letage, I., Raimbault, P., Waldman, R., Bouin, M.-N., Giordani, H., Caniaux, G., Somot, S., Ducrocq, V., Conan, P., 2018. Multiscale observations of deep convection in the northwestern Mediterranean Sea during winter 2012–2013 using multiple platforms. Journal of Geophysical Research: Oceans 123 (3), 1745–1776.

Thuróczy, C.E., Gerringa, L.J.A., Klunder, M.B., Middag, R., Laan, P., Timmermans, K.R., de Baar, H.J.W., 2010. Speciation of Fe in the eastern North Atlantic Ocean. Deep-Sea Research Part I-Oceanographic Research Papers 57 (11), 1444–1453.

Tovar-Sánchez, A., Rodríguez-Romero, A., Engel, A., Zäncker, B., Fu, F., Marañón, E., Pérez-Lorenzo, M., Bressac, M., Wagener, T., Triquet, S., Siour, G., Desboeufs, K., Guieu, C., 2020. Characterizing the surface microlayer in the Mediterranean Sea: trace metal concentrations and microbial plankton abundance. Biogeosciences 17 (8), 2349–2364.

Trezzi, G., Garcia-Orellana, J., Rodellas, V., Santos-Echeandia, J., Tovar-Sánchez, A., Garcia-Solsona, E., Masqué, P., 2016. Submarine groundwater discharge: a significant source of dissolved trace metals to the North Western Mediterranean Sea. Mar. Chem. 186, 90–100.

Tsimplis, M.N., Zervakis, V., Josey, S.A., Peneva, E.L., Struglia, M.V., Stanev, E.V., Theocharis, A., Lionello, P., Malanotte-Rizzoli, P., Artale, V., Tragou, E., Oguz, T., 2006. Chapter 4: Changes in the oceanography of the Mediterranean Sea and their link to climate variability. In: Lionello, P., Malanotte-Rizzoli, P., Boscolo, R. (Eds.), Developments in Earth and Environmental Sciences. Elsevier, pp. 227–282.

Twining, B.S., Rauschenberg, S., Morton, P.L., Vogt, S., 2015. Metal contents of phytoplankton and labile particulate material in the North Atlantic Ocean. Prog. Oceanogr. 137, 261–283.

UNEP, 2005. United Nations Environment Programme, Mediterranean Action Plan MED POL Transboundary diagnostic analysis (TDA) for the Mediterranean Sea. UNEP MAP Publication, Athens.

Van Cappellen, P., Powley, H.R., Emeis, K.C., Krom, M.D., 2014. A biogeochemical model for phosphorus and nitrogen cycling in the eastern Mediterranean Sea: part 1. Model development, initialization and sensitivity. J. Mar. Syst. 139, 460–471.

Van Geen, A., Boyle, E.A., Moore, W.S., 1991. Trace metal enrichments in waters of the Gulf of Cadiz, Spain. Geochimica et Cosmochimica Acta 55 (8), 2173–2191.

van Hulten, M., Middag, R., Dutay, J.C., de Baar, H., Roy-Barman, M., Gehlen, M., Tagliabue, A., Sterl, A., 2017. Manganese in the west Atlantic Ocean in the context of the first global ocean circulation model of manganese. Biogeosciences 14 (5), 1123–1152.

Velaoras, D., Krokos, G., Nittis, K., Theocharis, A., 2014. Dense intermediate water outflow from the Cretan Sea: a salinity driven, recurrent phenomenon, connected to thermohaline circulation changes. Journal of Geophysical Research: Oceans 119 (8), 4797–4820.

Vidussi, F., Claustre, H., Manca, B.B., Luchetta, A., Marty, J.-C., 2001. Phytoplankton pigment distribution in relation to upper thermocline circulation in the eastern Mediterranean Sea during winter. Journal of Geophysical Research: Oceans 106 (C9), 19939–19956.

Wagener, T., Guieu, C., Leblond, N., 2010. Effects of dust deposition on iron cycle in the surface Mediterranean Sea: results from a mesocosm seeding experiment. Biogeosciences 7 (11), 3769–3781.

Weber, T., John, S., Tagliabue, A., DeVries, T., 2018. Biological uptake and reversible scavenging of zinc in the global ocean. Science 361 (6397), 72–76.

Yilmaz, A.B., 2003. Levels of heavy metals (Fe, cu, Ni, Cr, Pb, and Zn) in tissue of Mugil cephalus and Trachurus mediterraneus from Iskenderun Bay, Turkey. Environmental Research 92 (3), 277–281.

Yu, H., Chin, M., Yuan, T., Bian, H., Remer, L.A., Prospero, J.M., Omar, A., Winker, D., Yang, Y., Zhang, Y., Zhang, Z., Zhao, C., 2015. The fertilizing role of African dust in the Amazon rainforest: a first multiyear assessment based on data from Cloud-Aerosol Lidar and Infrared Pathfinder Satellite Observations. Geophys. Res. Lett. 42 (6), 1984–1991.